UNIVERSIDADE ESTADUAL PAULISTA
"JÚLIO DE MESQUITA FILHO"
Campus de Botucatu

FCA
FACULDADE DE CIÊNCIAS AGRONÔMICAS
UNESP | BOTUCATU

RENATA TEIXEIRA DE ALMEIDA MINHONI

SOIL ORGANIC CARBON MONITORING IN AN IRRIGATED AGRICULTURE AREA

Botucatu

2021

RENATA TEIXEIRA DE ALMEIDA MINHONI

SOIL ORGANIC CARBON MONITORING IN AN IRRIGATED AGRICULTURE AREA

Thesis submitted to São Paulo State University (UNESP), School of Agriculture, Botucatu, to obtain the doctoral degree in Agronomy (Irrigation and Drainage).

Advisor: Dr. João Carlos Cury Saad

Co-Advisors: Dr. Daniele Zaccaria and

Dr. Elia Scudiero

Botucatu

2021

M664m

Minhoni, Renata Teixeira de Almeida
Monitoramento de carbono orgânico no solo em área agrícola irrigada / Renata Teixeira de Almeida Minhoni. -- Botucatu, 2021
77 p.

Tese (doutorado) - Universidade Estadual Paulista (Unesp), Faculdade de Ciências Agronômicas, Botucatu
Orientador: João Carlos Cury Saad
Coorientador: Daniele Zaccaria

1. Carbono orgânico do solo. 2. Irrigação. 3. Sensoriamento remoto. I. Título.

Sistema de geração automática de fichas catalográficas da Unesp. Biblioteca da Faculdade de Ciências Agronômicas, Botucatu. Dados fornecidos pelo autor(a).

Essa ficha não pode ser modificada.

UNIVERSIDADE ESTADUAL PAULISTA

Câmpus de Botucatu

CERTIFICADO DE APROVAÇÃO

TÍTULO DA TESE: MONITORAMENTO DE CARBONO ORGÂNICO NO SOLO EM ÁREA AGRÍCOLA IRRIGADA

AUTORA: RENATA TEIXEIRA DE ALMEIDA MINHONI
ORIENTADOR: JOÃO CARLOS CURY SAAD
COORIENTADOR: ELIA SCUDIERO
COORIENTADOR: DANIELE ZACCARIA

Aprovada como parte das exigências para obtenção do Título de Doutora em AGRONOMIA (IRRIGAÇÃO E DRENAGEM), pela Comissão Examinadora:

Prof. Dr. JOÃO CARLOS CURY SAAD (Participaçao Virtual)
Engenharia Rural e Socioeconomia / Faculdade de Ciências Agronômicas de Botucatu - UNESP

p/ Prof. Dr. RODRIGO MÁXIMO SÁNCHEZ ROMÁN (Participaçao Virtual)
Engenharia Rural e Socioeconomia / Faculdade de Ciências Agronômicas de Botucatu - UNESP

p/ Prof. Dr. DIEGO AUGUSTO DE CAMPOS MORAES (Participaçao Virtual)
Análise e Desenvolvimento de Sistemas / Faculdade Eduvale de Avaré

p/ Prof. Dr. JARBAS HONORIO DE MIRANDA (Participaçao Virtual)
Engenharia de Biossitemas / Escola Superior de Agricultura Luiz de Queiroz

p/ Prof. Dr. RUBENS DUARTE COELHO (Participaçao Virtual)
Engenharia de Biossistemas / Escola Superior de Agricultura Luiz de Queiroz

Botucatu, 04 de março de 2021

This thesis is dedicated to my family, for their endless support and encouragement.

ACKNOWLEDGMENTS

I am particularly grateful to my supervisor, Dr. João Carlos Cury Saad, for guiding me through the years of the doctoral program and supporting the achievement of this goal.

I am deeply thankful to my co-supervisors, Dr. Daniele Zaccaria and Dr. Elia Scudiero, for all the support and help since our first meeting. I was greatly inspired and motivated by their profound knowledge and enthusiasm for research.

I am truly thankful to Dr. Rodrigo Máximo Sánchez Román for his continuous guidance and advice throughout the entire process.

My sincere appreciation also goes to Dr. Célia Regina Lopes Zimback, who initially supervised and mentored me through the initial steps of my doctorate before her retirement.

I am also thankful to the National Council for Science and Technology (CNPq) for granting the doctoral scholarship (grant number: 140676/2017-1).

My sincere gratitude goes to the Institutional Program for Internationalization of Higher Education Institutions and Research Institutions (PrInt) by the Brazilian Federal Agency for Support and Evaluation of Graduate Education (CAPES) for the financial support (grant number: 88887.364471/2019-00) for my doctoral period at the University of California, Davis.

I also want to thank Abel Rodrigues Simões Júnior from “Olhos D’Água” farm for the support and for providing a soil dataset.

Thanks to my family for the unconditional support and patience through all these years.

ABSTRACT

There is a global growing interest in agricultural practices to increase soil organic carbon (SOC) to promote soil fertility, climate change mitigation, and food security. Therefore, SOC measuring and monitoring is a key step in agricultural and environmental projects. The first chapter of this study aimed to identify potential proxies for topsoil SOC in an agricultural area, characterized by the adoption of central pivot irrigation, reduced cultivation, crop rotation, and use of crop residues. Nine spectral indices were extracted from time-series Sentinel-2 satellite images of bare soil. Additionally, three topographic indicators were extracted from a digital elevation model (DEM). Linear regression models were generated between the spectral indexes and SOC, considering the soil sampled in 2019, and between topographic indicators and SOC. The spectral indices with the best performance were EVI2 (Enhanced Vegetation Index), NDVI (Normalized Difference Vegetation Index), MSAVI2 (Modified Soil-Adjusted Vegetation Index), and RVI (Ratio Vegetation Index), and the elevation was the best topographic indicator. After a seven-year study period (from 2012 to 2019), the area showed a significant increase in the topsoil SOC. The results of this research consolidate that the use of a multitemporal dataset can lead to more accurate identification of topsoil SOC proxies, instead of the use of a single date image. Two orchards were selected in the region of San Joaquin Valley, California (USA), having as the main objective of the second chapter characterize the multi-scale (tree scale and orchard scale) distribution of SOC and soil total nitrogen (STN) in micro-irrigated citrus orchards, grown under the same soil conservation practice. The first with Page mandarin (*Citrus reticulata*) in Strathmore, and the second with Washington navel orange (*Citrus sinensis*) in Ivanhoe. Both orchards are irrigated with micro-sprinklers, and pruning residues are disposed on the inter-rows. Soil samples were collected along transects, and each transect was divided into three sections: the first (α) located 0.6 m from the tree trunk, the second (β) 1.2 m from the trunk (approximately below the canopy projection), and the third (γ) located in the center of the inter-row. In each section single samples were collected at two soil layers, 0-0.05 m and 0.05-0.4 m. From 0 to 0.05 m in Strathmore, the average SOC concentrations in the β and γ sections and the STN concentration in the γ section showed no statistical difference with the orchard. Whereas, from 0.05 to 0.40 m and from 0 to 0.40 m there was no statistical difference between the sections and the orchard. In Ivanhoe, where the soil is more homogeneous, there was no significant difference between the sections and the orchard. The results of this study can support the elaboration of future SOC and STN monitoring projects in the region.

Keywords: Citrus orchard. Conservation practices. Remote sensing. Soil sampling. Spectral indices.

RESUMO

Há um crescente interesse global em práticas agrícolas que aumentem o carbono orgânico do solo (COS) para promover a fertilidade, a mitigação das mudanças climáticas e a segurança alimentar. Dessa maneira, a medição e monitoramento do COS é uma etapa muito útil em projetos agrícolas e ambientais. O primeiro capítulo deste estudo teve como objetivo principal a identificação de potenciais indicadores para o carbono orgânico presente na camada superficial do solo de uma área agrícola, caracterizada pela adoção de irrigação por pivô central, cultivo reduzido, rotação de culturas e utilização de resíduos de culturas. A partir de uma série temporal de imagens de solo exposto obtidas com o satélite Sentinel-2 foram extraídos nove índices espectrais. Também foram extraídos três indicadores topográficos a partir de um modelo digital de elevação (MDE). Foram gerados modelos de regressão linear entre os índices espectrais e COS, considerando o solo amostrado em 2019, e entre indicadores topográficos e o COS. Os índices espectrais de melhor desempenho foram EVI2 (*Enhanced Vegetation Index*), NDVI (*Normalized Difference Vegetation Index*), MSAVI2 (*Modified Soil-Adjusted Vegetation Index*) e RVI (*Ratio Vegetation Index*), e a elevação foi melhor indicador topográfico. Após um período de sete anos (2012-2019) de estudo, a área apresentou um aumento significativo no COS na camada superficial. Os resultados desta pesquisa consolidam que o uso de um conjunto de dados multitemporais pode levar a uma identificação mais precisa de indicadores de COS da camada superior do solo, ao invés do uso de imagem de uma única data. Foram selecionados dois pomares na região do Vale de San Joaquin na Califórnia (EUA), tendo como objetivo principal do segundo capítulo caracterizar a distribuição multi-escalar (escala de árvore e escala de pomar) de COS e nitrogênio total do solo (NTS) em pomares cítricos irrigados por microaspersão, cultivados sob a mesma prática de conservação do solo. O primeiro com *Page mandarin* (*Citrus reticulata*) em Strathmore, e o segundo com *Washington navel orange* (*Citrus sinensis*) em Ivanhoe. Ambos os pomares são irrigados com microaspersores e dispõem resíduos de poda nas entrelinhas. Foram coletadas amostras de solo ao longo de transectos, e cada transecto foi dividido em três seções: a primeira (α) localizada a 0,6 m do tronco da árvore, a segunda (β) a 1,2 m do tronco (aproximadamente abaixo da projeção da copa das árvores) e a terceira (γ) localizada no centro da entrelinha. Em cada seção foram coletadas amostras simples em duas camadas, em 0-0,05 m e em 0,05-0,4 m. De 0 a 0,05 m em Strathmore, as concentrações médias de COS nas seções β e γ e a concentração de NTS na seção γ não apresentaram diferença estatística em relação ao pomar. Enquanto que, de 0,05 a 0,40 m e de 0 a 0,40 m não houve diferença estatística entre as seções e o pomar. Em Ivanhoe, onde o solo é mais homogêneo, não houve diferença significativa entre as seções e o pomar. Os resultados deste estudo poderão subsidiar na elaboração de projetos futuros de monitoramento de COS e NTS na região.

Palavras-chave: Pomar de citros. Práticas conservacionistas. Sensoriamento remoto. Amostragem de solo. Índices espectrais.

SUMMARY

GENERAL INTRODUCTION

In the next 30 years there is an expected increase of 2 billion persons in the world's population, from currently 7.7 billion to 9.7 billion by 2050, and continuing to grow to around 10.9 billion by 2100 (UNITED NATIONS, 2019). It reveals an increased need for food production of about 70%, to meet the growing population demand until 2050, or approximately 100% if considered the developing countries (FAO, 2009). A current challenge is to accomplish food security through the rise in world food production (FRÓNA et al., 2019).

The irrigation of world agricultural lands is an essential key in food production, economic and rural development, and in the growth of job opportunities (ANGELAKIS et al., 2020). Experts recognized the crucial role of irrigation in the increment of food production (FAO, 2003). The irrigation-based agriculture can reduce the potential risks related to precipitation uncertainty, ensuring food security (PERRY et al., 2009) and stable crop production (SALAZAR; RAND, 2016).

Currently, over 60% of the global cereal production and 50% of the value of all crop products are due to irrigated agriculture (ANGELAKIS et al., 2020). An irrigated cropland produces about two and a half times more crop per hectare than a rainfed land (KENDALL; PIMENTEL, 1994). In Brazil, the average crop production in irrigated lands is at least 2.7 times greater relative to non-irrigated areas (FAO, 2017).

Globally, the area equipped for irrigation is 307.6 million hectares (Mha), of which around 69% is in Asia and 17% in America, and where China (62.4 Mha), India (61.9 Mha), and the United States of America (28.4 Mha) are the countries with the largest area (SIEBERT et al., 2013). California (4.2 Mha), Nebraska (3.6 Mha), and Texas (2.9 Mha) are the states with the largest areas equipped in the United States of America, where most of the area is irrigated with groundwater (FAO, 2020b). California supplies more than a third of the vegetables and two-thirds of fruits and nuts of the country, including almonds, pistachios, and grapes (CDFA, 2020).

Besides China, India, and the United States of America, Brazil is also among the ten countries with the largest equipped area for irrigation (FAO, 2020b). The estimated equipped area for irrigation in Brazil is around 6.95 Mha, of which 39% is in the Southeastern and 24% in the Southern regions of the country (ANA, 2017). Most of the irrigated area in the South region is by surface irrigation, due to rice production through food irrigation, whereas conventional sprinkler and central pivot irrigation are

the predominant systems in the Southeastern region (TESTEZLAF, 2017). The area for irrigation in Brazil has the potential to be expanded to 76,19 Mha, almost 11 times greater relative to the current area (ANA, 2017).

A global concern about the future increase of irrigated areas is the decrease in water availability, needed to supply agricultural and non-agricultural water demands. Additionally, climate change will affect the expansion and productivity of agricultural lands (irrigated or non-irrigated) due to the expected negative impact on water resources (TURRAL et al., 2011). Irrigation water is a crucial element for the agricultural development in the Mediterranean climate of California, where the precipitation is not regular and there is a shortage of available water (JOHNSON; CODY, 2015).

There are potential agricultural strategies to reduce the vulnerability towards the impacts of climate change. Considering farm and field scales, the adoption of agricultural practices, such as minimum or no-tillage, crop rotation, adoption of winter cover crops, and use of crop residues, can increase water infiltration and holding capacity, and improve soil health (Pathak et al., 2018). Crop residue practices tend to reduce soil water evaporation, improve the water use efficiency (MITCHELL et al., 2012; HATFIELD; DOLD, 2019), support the maintenance of organic carbon and nutrients in the soil (GHIMIRE et al., 2017). Minasny and McBratney (2017) reported, through a literature review, that a 1% mass increase in organic carbon (or 10 g C kg^{-1}), promoted an average increase of 1.16% in the available water capacity (1.16 mm H_2O 100 mm $soil^{-1}$).

Soil organic carbon (SOC) is one of the major indicators of the sustainability of agricultural lands (STELLA et al., 2019). SOC provides several benefits to soil health, improving aggregation and structure, biodiversity and biotic activity, nutrients and water retention, and decrease the risks of soil erosion and degradation (LAL, 2004). Furthermore, increasing SOC can improve the resilience of the soil towards drought events (LAL, 2016). Enhancing SOC and soil health are pertinent to the achievement of various sustainable development goals (SDG), such as climate action (SDG 13), live on land (SDG 15), and zero hunger (SDG 2). It would support climate change adaptation and mitigation, promote food security, and contribute specifically to SDG 15.3, by combating desertification and restoring degraded soils (RUMPEL et al., 2020).

The perspective of measuring, monitoring, reporting, and verifying SOC is a critical action for any agricultural project related to soil carbon, and climate change, supporting

management decisions (FAO, 2020a). An efficient SOC monitoring at the farm scale is essential to verify the soil quality framework and provide perspectives and incentives for climate mitigation (DELUZ et al., 2020). There is still a necessity that should be assessed or reviewed to better understand the agricultural management effects on SOC (CHENU et al., 2019). Besides the conventional methods for SOC monitoring, which are expensive, labor-intensive, and time-consuming (MIRCHOOLI et al., 2020), remote sensing techniques can offer a rapid, and low-cost alternative to estimate variables for different soil monitoring purposes (ANGELOPOULOU et al., 2019).

This thesis presents research on SOC characterization and monitoring in two different study areas, in a subtropical area in Brazil and a temperate area in the USA. The objectives of the first chapter of this research were to use remote sensing data to identify potential proxies for topsoil SOC and monitor SOC changes over time in an agricultural area, characterized by the adoption of central pivot irrigation, reduced cultivation, crop rotation, and utilization of crop residues (straw). The main objective of the second chapter was to characterize the multi-scale soil spatial patterns of organic carbon and total nitrogen over micro-irrigated citrus orchards, grown under the same soil conservation practice.

CHAPTER 1[1]

MULTITEMPORAL SATELLITE IMAGERY ANALYSIS FOR SOIL ORGANIC CARBON ASSESSMENT IN AN AGRICULTURAL FARM IN SOUTHEASTERN BRAZIL

Renata Teixeira de Almeida Minhoni [a,*], Elia Scudiero [b,c], Daniele Zaccaria [d], João Carlos Cury Saad [a]

[a] São Paulo State University, São Paulo State University (UNESP), School of Agronomical Sciences, Campus Botucatu, Av. Universitária, 3780, Botucatu, SP, 18610-034, Brazil.
[b] University of California, Riverside, Department of Environmental Sciences, 900 University Ave., Riverside, CA 92521, USA.
[c] United States Department of Agriculture – Agricultural Research Service, U.S. Salinity Laboratory, 450 West Big Springs Rd., Riverside, CA 92507, USA.
[d] Department of Land, Air and Water Resources, University of California, Davis, CA 95616, USA.
* Corresponding author.

E-mail addresses: renata.minhoni@unesp.br (R.T.A. Minhoni), elia.scudiero@ucr.edu (E. Scudiero), dzaccaria@ucdavis.edu (D. Zaccaria), joao.saad@unesp.br (J.C.C. Saad).

HIGHLIGHTS

- Multitemporal imagery percentiles improved the detection of soil organic carbon.
- Spatial covariates were used to compare different soil sampling schemes.
- Organic carbon content increased over seven years of soil conservation practices.

ABSTRACT

Soil organic carbon (SOC) has a crucial role for soil health. However, large datasets needed to accurately assess SOC at high resolution across scales are labor-intensive and expensive. Therefore, ancillary geodata, including remote sensing spectral indices

[1] This chapter follows the guidelines of the journal “Science of the Total Environment”.

(SIs) and topographic indicators (TIs) have been proposed as spatial covariates. Reported relationships between SOC and SIs are erratic, possibly because single-date SIs do not accurately capture SOC spatial variability due to transient confounding factors in the soil (e.g., moisture). However, multitemporal SI data analysis may lead to noise reduction in SOC-SI relationships. Therefore, this study aimed at: i) comparing single-date versus multitemporal SIs (derived from Sentinel-2 imagery from 2018 through 2020) for assessment of topsoil (0-0.2 m) SOC (sampled in April 2019) in two agricultural fields in southeastern Brazil; ii) comparing the performance of SIs and TIs (derived from Topodata); and iii) using viable SIs and TIs to monitor SOC changes over time. Single-date SIs were not reliable proxies for topsoil SOC at the study sites. For most of the tested SIs, multitemporal data analysis produced accurate proxies for SOC; e.g., for the Normalized Difference Vegetation Index, the 4.5th multitemporal percentile predicted SOC with an R^2 of 0.64. The best TI was elevation (ranging from 643 to 684 m) with an R^2 of 0.70. Soil samples collected in 2012 and 2016 were on a different grid than in 2019. The multitemporal SI and elevation maps indicated that the different sampling schemes were all representative of the topsoil SOC distribution of the entire study area. From 2012 through 2019, topsoil SOC increased from 19.3 to 24.1 g kg^{-1}. The ratio between topsoil (0-0.2 m) and subsoil (0.2-0.4 m) SOC decreased from 1.7 to 1.1. Further testing of the proposed multitemporal SI analysis is necessary to confirm its reliability for SOC assessment in the watershed and state.

Keywords: Sustainable agriculture, crop rotation, reduced tillage, remote sensing, Sentinel-2, spectral indices.

GRAPHICAL ABSTRACT

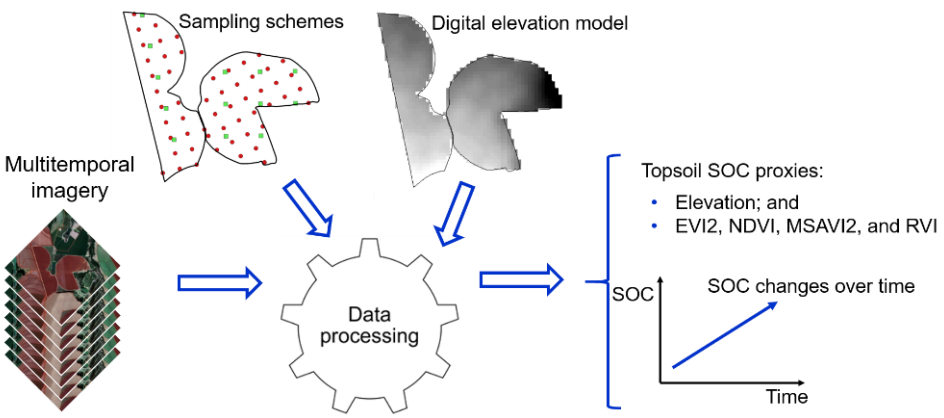

1.1 INTRODUCTION

The oceanic and terrestrial ecosystems are two of the main global carbon pools. The largest global pool is the oceanic, and the largest terrestrial pool is the soil, with an estimated 39,000 Pg and 2,200 Pg of carbon, respectively (Batjes, 1996). The soil organic carbon (SOC) pool is about 1,505 Pg to 1.0 m and 677 Pg to 0.3 m depth (Lal, 2018). Estimates of the soil inorganic carbon (SIC) range from 695 to 748 Pg to 1.0 m and 222 to 245 Pg to 0.3 m depth (Batjes, 1996). The SIC pool consists of carbonates (i.e. calcite, dolomite, and gypsum) and it affects the global carbon cycle, but with lower intensity than the SOC pool (Lal, 2004).

The SOC pool consists mainly of residues from plant, animal, and microbial biomass at different stages of decomposition (Lal, 2018). It is considered a keystone of agricultural systems, as it is a driver of soil fertility and structure (Liang et al., 2019). SOC helps to promote nutrient cycling, soil structure, water storage, microorganism activity, and biodiversity (Tautges et al., 2019).

Soils can act either as a source or as a sink of carbon, depending on climate conditions, biomass input, and management (Zomer et al., 2017). Small changes in SOC can strongly affect atmospheric CO_2 concentrations (Lal, 2018; Liang et al., 2019). As such, SOC sequestration is considered a possible strategy for climate change mitigation (Huang et al., 2019). Increasing SOC pool rearranges atmospheric CO_2 into a long-lived organic pool, improving soil health and resilience, compensating for the gas emissions, and mitigating the effects of climate change (Tautges et al., 2019).

Land management practices that enhance SOC storage in agricultural systems include conservation tillage, crop rotation, residue retention, cover cropping, fertility management, and addition of amendments (Lal, 2018; Paustian et al., 2016). Retention of crop residues, no-till, and reduced tillage are soil conservation practices that have been widely adopted to increase soil health and reduce the adverse environmental impacts generated by the intensive farming system (Li et al., 2020). Conservation agriculture practices tend to benefit aspects of soil health, increasing carbon storage and biodiversity, and improving nutrient cycling (Norris et al., 2018). Besides improving soil moisture and crop productivity, irrigation practices can also lead to an increase in SOC (Trost et al., 2013). Huynh et al. (2019) observed that irrigation is the major factor influencing maize biomass yield, followed by tillage, and crop

rotation. Irrigation provides water to meet crop transpiration requirements, and transpiration leads to the production of crop biomass (Perry et al., 2009), thus leading to increases in farmers' income and soil carbon inputs.

Conservation tillage is the use of specific tillage practices that reduce soil disturbance compared with conventional tillage, thus promoting soil and water conservation (Claassen et al., 2018). Conservation tillage, which includes reduced tillage and no-till, covers at least 30% of the soil surface with crop residue, while conventional tillage covers less than 15% of the soil surface with residue (Eskandari et al., 2016). Although some evidence showed that adoption of no-till (NT) in croplands tends to accumulate SOC in the top surface layers, whereas conventional tillage (CT) tends to increase SOC deeper into the soil profile, many studies showed divergent results in SOC storage between NT and CT (Angers and Eriksen-Hamel, 2008).

Spatial and temporal variability of SOC is related to land use, climate, agricultural management, topographic variables, soil type (Mirchooli et al., 2020), and annual biomass-C inputs (Mishra et al., 2010). SOC should be assessed across multiple scales to meet the needs of different stakeholders, such as farmers (field to farm-scale maps) and policy makers (regional to global-scale maps) (Vaudour et al., 2019). Conventional methods for SOC monitoring at the field scale include extensive field sampling and laboratory analysis, but this process is time-consuming, demands intensive labor, and it is costly (Mirchooli et al., 2020; Chen et al., 2020). Less expensive SOC quantification is required by the rising demand from the agricultural community and to obtain high-resolution repositories at farm and broader scales (Padilha et al., 2020).

Remote sensing is a recognized technology that can provide a rapid, efficient, and inexpensive method to assess SOC in bare soils (Castaldi et al., 2019a, Kumar et al., 2017; Xu, et al., 2017). Products from remote sensing can generate a spectral reference base for soil properties, as an alternative to the expensive traditional field sampling and analysis (Castaldi et al., 2019a). The soil spectral reflectance is an integrative property derived from inherent characteristics, such as water content, surface roughness, texture, organic matter (SOM), and minerals (Ymeti et al., 2019). Generally, the higher is the soil moisture or the SOM content, the higher is the absorption of light and, consequently, the higher is the soil color and the lower is the soil reflectance (Jensen, 2007). Similarly, the soil color, as a component of SOM, also becomes darker with the increase in SOC. Therefore, images of areas taken with dry

soil can help reduce the effects of soil moisture on soil reflectance (Angelopoulou et al., 2019). Soil reflectance in the visible near-infrared and shortwave infrared (VIS-NIR-SWIR) wavelengths, which range from 0.4 to 2.5 μm, is highly influenced by SOC content (Vaudour et al., 2019). Satellite images can enable to evaluate SOC changes over time at locations that do not have soil monitoring or soil legacy data (Grinand et al., 2017), thus representing an essential technology for agricultural management policies and practices (e.g., Padilha et al., 2020).

There are remote sensing satellite platforms providing imagery with different spatial, temporal, and spectral resolutions, which may allow SOC prediction with varying levels of accuracy (Wang et al., 2020). Multispectral satellites, such as Sentinel-2, can provide a high-quality capacity to assess SOC similar to that allowed by upcoming hyperspectral satellites (Castaldi et al., 2019b). The Copernicus Sentinel-2 mission provides free imagery, a high revisit time (five days at the Equator), and thirteen spectral bands (four with 10 m, six with 20 m, and three with 60 m of spatial resolution) (European Space Agency, 2015). Spectral indices from satellite images can reflect vegetation variations and can be used for monitoring soil properties inferred from reflectance in specific spectral bands, such as SOC (e.g., Zhang et al., 2019). However, only a few studies tested the applicability of Sentinel-2 imagery to assess SOC, such as the studies conducted by Castaldi et al. (2016), Kumar et al. (2017), Gholizadeh et al. (2018), Castaldi et al. (2019b), Valdour et al. (2019), and Žížala et al. (2019). Moreover, terrain attributes, which can be derived from a digital elevation model (DEM), are covariates being broadly used in SOC studies (Fathololoumi et al., 2020; Kunkel et al., 2019).

Gholizadeh et al. (2018) used spectral indices derived from single-date Sentinel-2 data to monitor and map SOC and soil texture in agricultural areas, and the chosen satellite data were close to the soil sampling date with bare soil condition. Kumar et al. (2018) applied spectral indices obtained from a single-date ASTER image to assess SOC in a heterogeneous study area. These authors also utilized a satellite image taken close to the soil sampling campaign, as Gholizadeh et al. (2018) did. Santos et al. (2014) derived spectral indices from a single-date Landsat 5 data of September 2011 to estimate SOC in different soil classes. Since the soil sampling was conducted between July and September 2012, the authors justified selecting a satellite image from a different period due to imagery availability until 2011. Although many studies utilized single-date satellite data to assess SOC, we hypothesize that more accurate

assessment can be obtained from the use of multitemporal satellite data, as it would reduce space-time specific random error in the relationship between SOC and parameters derived from satellite data.

The main objectives of the present study were: 1) comparing single-date versus multitemporal data analysis for SOC assessment; 2) evaluating the performance of spectral indices coupled with terrain elevation products, which are known to be good estimators for SOC; and 3) once some reliable proxies for spatial variability of SOC are identified, use them to assess SOC changes in the study area over time.

1.2 MATERIAL AND METHODS

1.2.1 Description of the study area

São Paulo state is divided into 22 Water Resources Management Units (also known as “UGRHI” in the state of São Paulo). Each UGRHI belongs to a watershed and has its identification number and name. The UGRHI No. 14 - Alto Paranapanema is extensively characterized by field crops irrigated mainly with center-pivots (Ferreira et al., 2016). About 48.57% of the irrigated area of the São Paulo state is located within the Paranapanema River basin, with approximately 45.27% belonging to the Alto Paranapanema sub-basin (Landau et al., 2014). Here, a study area consisting of two neighboring fields was selected.

The study area is in a commercial farm located at Itaí (SP), between the latitudes 23°32’26”S and 23°35’38”S and the longitudes 48°54’16”W and 48°51’39”W. The present research work was conducted on the cropland irrigated by two center-pivots, which is divided into site A (49 ha) and site B (64 ha) as illustrated in Fig. 1.

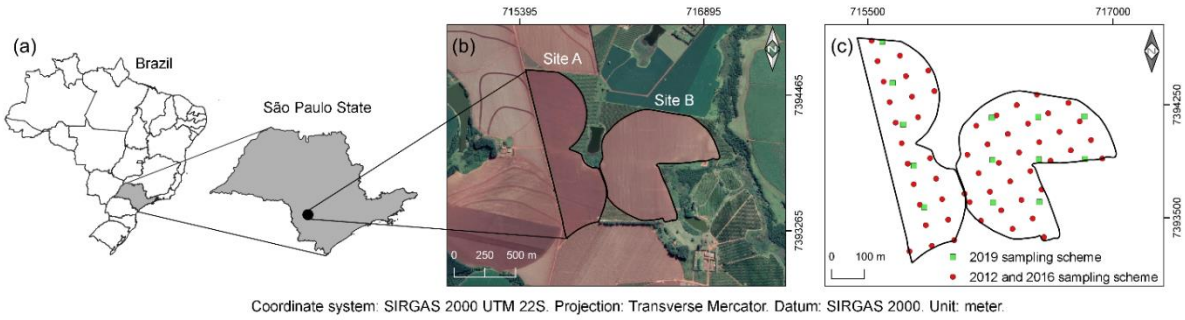

Fig. 1. Overview of the study area with the indication of a) the geographic location; b) subdivision in two study sites (A and B) from Google Earth picture (2019); c) soil sampling schemes of 2012-2016 and 2019.

Before 2010, the study fields were managed with conventional tillage. Since 2010, both the sites have been managed with a combination of conservation agricultural practices, including reduced tillage and crop rotation. Both the sites were irrigated with center-pivots. In addition, the residues from the previous crop were left on the soil surface. Bean (*Phaseolus vulgaris* L.), soybean (*Glycine max* L.), corn (*Zea mays* L.), and cotton (*Gossypium hirsutum* L.) were the four main crops grown at the study sites. Table S1 in the Supplementary Material provides an example of 5-year crop rotation at each study site, with information about the individual crops, as well as the showing date and the harvest.

The soil in the study sites is classified as Ferrasol (IUSS Working Group WRB, 2015), which is equivalent to a Latosol (SiBCS, 2018). It is characterized by average values of 65.2% of clay, 25.9% of silt, and 8.9% of sand at the topsoil layer (0-0.2 m), and 68.5% of clay, 22.6% of silt, and 8.9% of sand at the subsoil layer (0.2-0.4 m) (Souza et al., 2016).

1.2.2 SOC dataset

The land manager provided the soil legacy dataset (existing soil dataset) that was used in the present study. The field dataset was produced with the purpose of monitoring soil fertility. Soil samples were collected in 2012, 2016, and 2019. Six disturbed samples were collected within a 40 m radius to create a composite sample per location. The sampling scheme of 2012 and 2016 was the same (Fig. 1c). Due to the high costs of sampling and analysis, the sampling scheme of 2019 consisted of fewer sampling locations (Fig. 1c). Table 1 shows the details of the soil sampling schemes at the study sites. A variety of parameters were assessed through the soil sampling survey, including organic matter, pH, cation exchange capacity, phosphorus, potassium, calcium, and magnesium. However, only organic matter (SOM) data were considered for the present study. The SOM analyses were conducted following the Walkley-Black methodology (Walkley and Black, 1934).

Table 1
Information on the soil sampling schemes.

Location	October 2012			July 2016			April 2019		
	n	Sampling density	Soil layer (m)	*n*	Sampling density	Soil layer (m)	*n*	Sampling density	Soil layer (m)
Site A	24	1 per 2.04 ha	0-0.2 and 0.2-0.4	24	1 per 2.04 ha	0-0.2	5	1 per 9.80 ha	0-0.2 and 0.2-0.4
Site B	31	1 per 2.06 ha	0-0.2 and 0.2-0.4	31	1 per 2.06 ha	0-0.2	8	1 per 8.00 ha	0-0.2 and 0.2-0.4

n = number of sampling locations.

The equation 1 was used to derive SOC from the soil organic matter data. In Eq. 1, the conversion factor of 1.724 is based on the assumption that organic matter contains approximately 58% of organic carbon (Yigini et al., 2018). This conversion factor, known as the van Bemmelen factor, has been used as a universal factor due to the high costs of equipment and its maintenance required to measure soil organic carbon (Heaton et al., 2016).

$$SOC = 0.58\ x\ SOM \quad or \quad SOC = \frac{SOM}{1.724} \tag{1}$$

1.2.3 Remote sensing data source and processing

Ten cloud-free Sentinel-2 Level-2A scenes with bare soil conditions were downloaded from the Copernicus open access hub (https://scihub.copernicus.eu/). In this study, bare soil is assumed as the soil with no active or growing vegetation and with the possible presence of crop residues that were left out onto the soil surface from the previous crop after harvest. The processing of Level-2A includes an atmospheric correction applied to Top-Of-Atmosphere (TOA) Level-1C products (European Space Agency, 2015). The downloaded multitemporal imagery dataset included one image from 2018, eight from 2019, and one from 2020. The imagery captured bare soil at both the sites on three scenes, and individually for site A only over four scenes, and for site B only over three scenes.

The Sentinel-2 mission is a combination of two identical satellites (Sentinel-2A and Sentinel-2B), offering a five-day revisit time. The MSI (Multispectral Instrument) is on-board of each satellite, providing Earth's reflectance imagery over 13 spectral bands.

The multi-spectral information from Sentinel-2 used in this study included: blue (B2, 0.490 µm), green (B3, 0.560 µm), red (B4, 0.665 µm), and near-infrared (B8, 0.842 µm) with 10 m of spatial resolution, and shortwave infrared 1 (B11, 1.610 µm) with 20 m of spatial resolution.

Nine spectral indices were calculated with the reflectance from these bands to detect proxies for SOC and improve its prediction (see Table 2 for definitions and references). The selected indices were: Canopy Response Salinity Index (CRSI), Difference Vegetation Index (DVI), Enhanced Vegetation Index 2 (EVI2), Modified Soil-Adjusted Vegetation Index 2 (MSAVI2), Normalized Difference Vegetation Index (NDVI), Normalized Difference Water Index (NDWI), Renormalized Difference Vegetation Index (RDVI), Ratio Vegetation Index (RVI), and Soil Organic Carbon Index (SOC Index). The analytical formulations to derive these spectral indices, as well as those based on the Sentinel-2 bands, are presented in Table 2. To produce NDWI, B11 was resampled from 20-m to 10-m pixel resolution using the ESA's Sentinels Application Platform (SNAP) open-source software.

Table 2
Spectral indices derived from Sentinel-2 multispectral bands.

Spectral index[a]	Formulation	Formulation based on Sentinel-2	Reference
CRSI	$\sqrt{\frac{(NIR.RED)-(GREEN.BLUE)}{(NIR.RED)+(GREEN.BLUE)}}$	$\sqrt{\frac{(B8.B4)-(B3.B2)}{(B8.B4)+(B3.B2)}}$	Scudiero et al. (2014)
DVI	$NIR-RED$	$B8-B4$	Tucker (1979)
EVI2	$\frac{2.4.(NIR-RED)}{(NIR+RED+1)}$	$\frac{2.4.(B8-B4)}{(B8+B4+1)}$	Jiang (2008)
MSAVI2	$\frac{2.NIR+1-\sqrt{(2.NIR+1)^2-8.(NIR-RED)}}{2}$	$\frac{2.B8+1-\sqrt{(2.B8+1)^2-8.(B8-B4)}}{2}$	Qi et al. (1994)
NDVI	$\frac{(NIR-RED)}{(NIR+RED)}$	$\frac{(B8-B4)}{(B8+B4)}$	Rouse et al. (1974)
NDWI	$\frac{(NIR-SWIR)}{(NIR+SWIR)}$	$\frac{(B8-B11)}{(B8+B11)}$	Gao (1996)
RDVI	$\frac{(NIR-RED)}{\sqrt{(NIR+RED)}}$	$\frac{(B8-B4)}{\sqrt{(B8+B4)}}$	Roujean and Breon (1995)
RVI	$\frac{NIR}{RED}$	$\frac{B8}{B4}$	Rondeaux et al. (1996)
SOC Index	$\frac{BLUE}{(RED.GREEN)}$	$\frac{B2}{(B4.B3)}$	Thaler et al. (2019)

[a] CRSI: Canopy Response Salinity Index, DVI: Difference Vegetation Index, EVI2: Enhanced Vegetation Index 2, MSAVI2: Modified Soil-Adjusted Vegetation Index 2, NDVI: Normalized Difference Vegetation Index, NDWI: Normalized Difference Water Index, RDVI: Renormalized Difference Vegetation Index, RVI: Ratio Vegetation Index, and SOC Index: Soil Organic Carbon Index.

We compared the ability of remotely-sensed indices to estimate SOC to that of topographic data, which has been widely used to model SOC dynamics (Wang et al., 2018b).

A 30 m resolution digital elevation model (DEM) was acquired from Topodata (http://www.dsr.inpe.br/topodata/), which is a product of a refinement process of SRTM (Shuttle Radar Topography Mission) elevation data from 3” to 1” vertical resolution (Valeriano and Rossetti, 2012). The DEM was used to generate three standardized terrain attributes: elevation, slope, and TWI (Topographic Wetness Index). TWI was calculated according to Equation 2 (Moore et al., 1993).

$$TWI = \ln \frac{A_s}{\tan \beta} \quad (2)$$

where A_s is the specific catchment area (or contributing area) per unit contour length (m^2 m^{-1}), and β the local slope. In this study, β is the slope gradient of the area commanded by the center-pivot. TWI works as a mass balance, where A_s describes the trend to receive water, and β the trend to discharge water (Mattive et al., 2019). TWI represents the tendency of each unit (pixel) to accumulate water according to the relief (Sena et al., 2020).

The nine spectral indices and the three terrain attributes were tested for their performance as proxies for SOC at the study area.

1.2.4 Data analysis

The correlations between topsoil SOC (2019 dataset) and geospatial data (i.e., spectral indices and topography) at the two study sites were investigated using linear regression analyses. Notice that the use of regressions using different slope and/or intercept values for the two fields. These analyses returned non-significant differences in slope and intercept values between the two sites indicating that single regression models were adequate to describe the investigated relationships across the two sites. The regression's coefficient of determination (R^2), intercept and slope values, slope's p-values were used to infer the feasibility of spectral indices and topography as proxies for SOC.

The performance of spectral indices from single satellite scenes and multitemporal stacks as proxies for SOC was evaluated. For the multitemporal analysis, the available imagery was snapped onto a common grid. Then, at each grid location, spectral index values were ranked from lowest to highest. The percentile (α) of these temporal distributions were such that values of $\alpha = 0$ and $\alpha = 1$ corresponded to the lowest and highest values across the multitemporal imagery stack at each grid location. Then, regressions using spectral index values from the same α levels as explanatory variables were evaluated. The spectral indices' values corresponding to the entire $0 \leq \alpha \leq 1$ temporal distribution were estimated using the "PERCENTILE.INC" function in Microsoft Office Excel 2016 (Redmond, WA, USA). For each spectral index, the α value returning the linear regression with the strongest goodness-of-fit (i.e., lowest total sum of squares) with SOC was identified through Generalized Reduced Gradient nonlinear optimization using Solver (Frontline Systems, Incline Village, NV, USA) in Excel.

Additionally, the robustness of the selection of α was tested using leave-one-out (LOO) resampling (i.e., Jackknifing). This was done by systematically leaving out each observation from the dataset (i.e., 2019 topsoil SOC) and selecting the best α for the regression between SOC and the spectral indices. The average and standard deviation of the resulting array of α values were then calculated. Ideally, LOO average α value should be close to the whole-dataset model calibration value and therefore have a small standard deviation.

Additionally, the best proxies for SOC derived from the geospatial data were used to verify if the two sampling schemes are comparable. The comparisons between the SOC for the sampling schemes and the best proxies were performed using an Analysis of Variance (ANOVA) (*p-value* < 0.05). The three different years of soil sampling were compared to detect changes in SOC. The two sites, considered individually and together, were compared using a Wilcoxon test for paired samples, in case of equal sampling schemes, and a Kruskal-Wallis rank test (*p-value* < 0.05), for different sampling schemes condition. A Pearson correlation analysis was performed to evaluate the relationship between subsoil SOC changes and topsoil SOC changes over time. This analysis aimed at understanding what can be inferred about subsoil SOC changes from the topsoil SOC data.

All the data analysis was performed using R software (R Core Team, 2020) and Microsoft Office Excel 2016 (Redmond, WA, USA).

1.3 RESULTS AND DISCUSSION

1.3.1 Spectral indices

1.3.1.1 Analysis for single date

The relationships between topsoil SOC (2019 dataset) and the selected spectral indices were analyzed according to the significance of the regression slope for all imagery acquisition dates (Fig. 2). None of the selected spectral indices returned significant correlations with SOC on the dates closest to the soil sampling time (April 2019). However, the regression slopes for all spectral indices changed remarkably over time. When significant, the relationships between SOC and DVI, EVI, MSAVI2, NDVI, RDVI, and RVI were negative, whereas those for NDWI and SOC Index were positive. CRSI never returned significant correlations with SOC. EVI2, MSAVI2, NDVI,

and RVI showed the strongest single-date correlations ($p<0.01$) across all indices on August 13, 2019. Generally, most significant ($p<0.05$) correlations were observed in June, July, and August 2019, during the winter period. Brazil's winter is a dry season that goes from June to September, whereas the summer is a rainy season that starts in December and ends in March. In 2019, a weather station near the study area (Paranapanema) recorded a mean monthly precipitation of 208.5 mm in January, 98.2 mm in June, 75.0 mm in July, and 5.2 mm in August (CIIAGRO, 2020). Our results suggest that erratic correlations with SOC are likely to be observed when using spectral indices from a single date. Such inconsistencies may be due to a variety of site- and time-specific confounding factors. The current understanding of remote sensing imagery and the relationships with soil property indicates that often multiple factors are influencing the remote sensing imagery (Xu et al., 2018), i.e., various factors having different spatial patterns may be captured by the remote sensing imagery. The relationship between a target soil variable, such as the topsoil SOC for this study, and spectral indices from remote sensing can be described as a spatial linear model for which the soil property is the dependent variable, the spectral index is the explanatory variable, and the error is a spatial random component (Scudiero et al., 2018; Xu et al., 2018). To best describe the spatial variability of the target soil variable, the magnitude of the spatial random error should be minimized. At the sites considered for the present study, the confounding factors contributing to the spatial random error probably included soil moisture, surface roughness, and the presence of plant stocks on the soil surface. The surface roughness of soils is described as irregularities over the surface, which can be produced by texture, size of aggregates, and soil management practices (Thomsen et al., 2015). The two study sites are next to each other and have the same soil type. The two sites were also under very similar farming management practices. Therefore, (surface) soil moisture may have been the main confounding factor contributing to the changes in the SOC relationship with spectral indices over time.

Published research on SOC relationships with spectral indices by using a single (concurrent or near in time) satellite imagery show very inconsistent results, most likely because the presence of confounding random errors in such relationships was not considered or tested. Gholizadeh et al. (2018) found a positive correlation between SOC and NDVI by using single-date Sentinel-2 data, differing from our results, and a negative correlation for MSAVI2 and RVI, in agreement with the results of this study. Kumar et al. (2018) investigated the effect of eight predictor variables for SOC using a

single-date ASTER satellite image. The same authors found out that NDVI produced a positive and the best correlation with SOC, which was due to the vegetation condition of the study area. Nevertheless, Zhang et al. (2019) derived NDVI from Landsat-8 multitemporal data and observed that this relationship goes from negative to positive, but also indicated that most images showed a negative correlation between SOC and NDVI. Their research work indicated that SOC cannot be predicted by using a single date NDVI image, which is consistent with the findings from the present study. When using spectral indices from a single-date, erratic correlations with SOC are likely to be obtained. Instead, multitemporal spectral indices analyze extra information regarding the study objective and result in a more robust approach (Zhang et al., 2019). These finding may be applied not only for NDVI, but also for other indices (i.e., EVI2, MSAVI2, and RVI), as illustrated in Fig. 2.

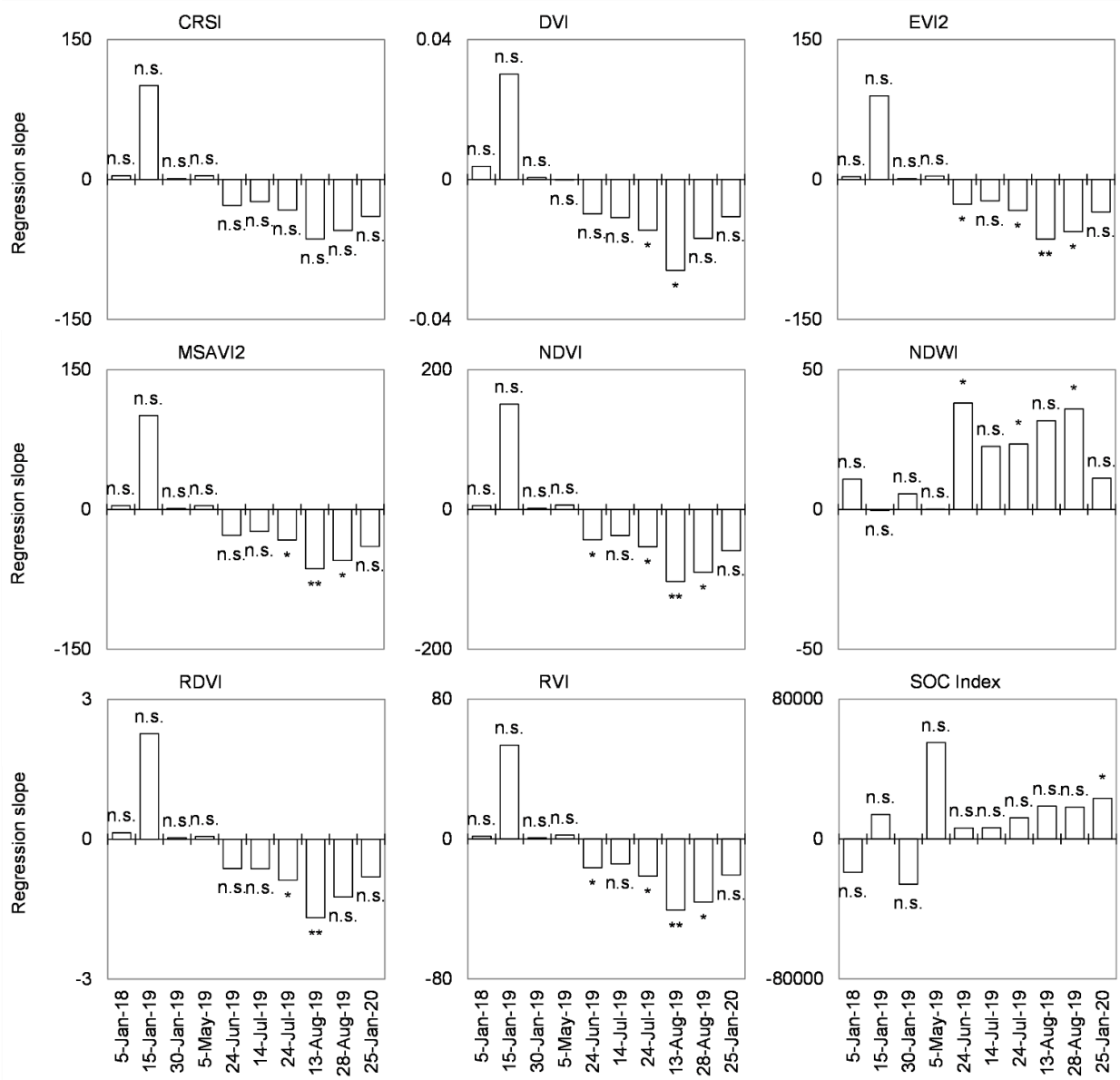

Fig. 2. Slope values of the linear regression between topsoil SOC (2019 dataset) and single date Sentinel-2 spectral indices. n.s.: non-significant (p-value ≥ 0.05), *: significant at p-value < 0.05, and **: significant at p-value < 0.01. CRSI: Canopy Response Salinity Index, DVI: Difference Vegetation Index, EVI2: Enhanced Vegetation Index 2, MSAVI2: Modified Soil-Adjusted Vegetation Index 2, NDVI: Normalized Difference Vegetation Index, NDWI: Normalized Difference Water Index, RDVI: Renormalized Difference Vegetation Index, RVI: Ratio Vegetation Index, and SOC Index: Soil Organic Carbon Index.

1.3.1.2 Spectral indices time series analysis

The key to minimizing the effect of spatial random error in the relationships between spectral indices and SOC may be via multitemporal remote sensing data analysis (ZHANG et al., 2019), as shown for other soil properties, such as salinity (Scudiero et

al., 2015) and heavy metals (Liu et al., 2018). The strength of the relationships between topsoil SOC (2019 survey) for selected α values of all spectral indices is shown in Fig. 3. Low p-values indicate strong relationships. When $p<0.05$, relationships are significant. In Fig. 3, for each index-SOC regression, the best α value is indicated with a label.

The strength of the SOC relationships with the spectral indices varied widely when different α values were used. All indices except CRSI showed significant ($p<0.05$) relationships with SOC. EVI2, MSAVI2, NDVI, and RVI yielded the strongest relationships with SOC. These four indices returned stronger relationships with different α values and were considered for further analyses. The strongest relationships for these four indices were observed around α values in the 0.039 to 0.049 range (Table 3). The four best spectral indices selected in this study use only red and near-infrared bands in their mathematical formulation. The soil spectral response is high in the red and near-infrared bands (Xue and Su, 2017), but it is also affected in the shortwave infrared region (Castaldi et al., 2016). SOM is spectrally active throughout the visible and near-infrared spectra, and the range across the shortwave infrared region has also been observed to correlate with SOM (Pearlshtien and Ben-Dor, 2020). Angelopoulou et al. (2020) indicated that the reflectance from the VIS-NIR-SWIR (visible-near infrared-shortwave infrared) spectral region (0.4-2.5 µm) is an important information that can be used to assess SOM and SOC. Particularly, the wavelength around 0.664 µm is an important region associated with SOM (Ben-Dor et al., 1997). The spectral reflectance around 0.664 µm is close to the spectral range from the red band (B4) of Sentinel-2, which goes from 0.650 to 0.680 µm (central wavelength = 0.665 µm). Castaldi et al. (2019b) also used Sentinel-2 data to predict SOC in croplands. These authors reported that the red and the near-infrared bands were more important than the shortwave infrared band in one of their study areas, where the mean SOC estimated was 26.7 g kg^{-1}.

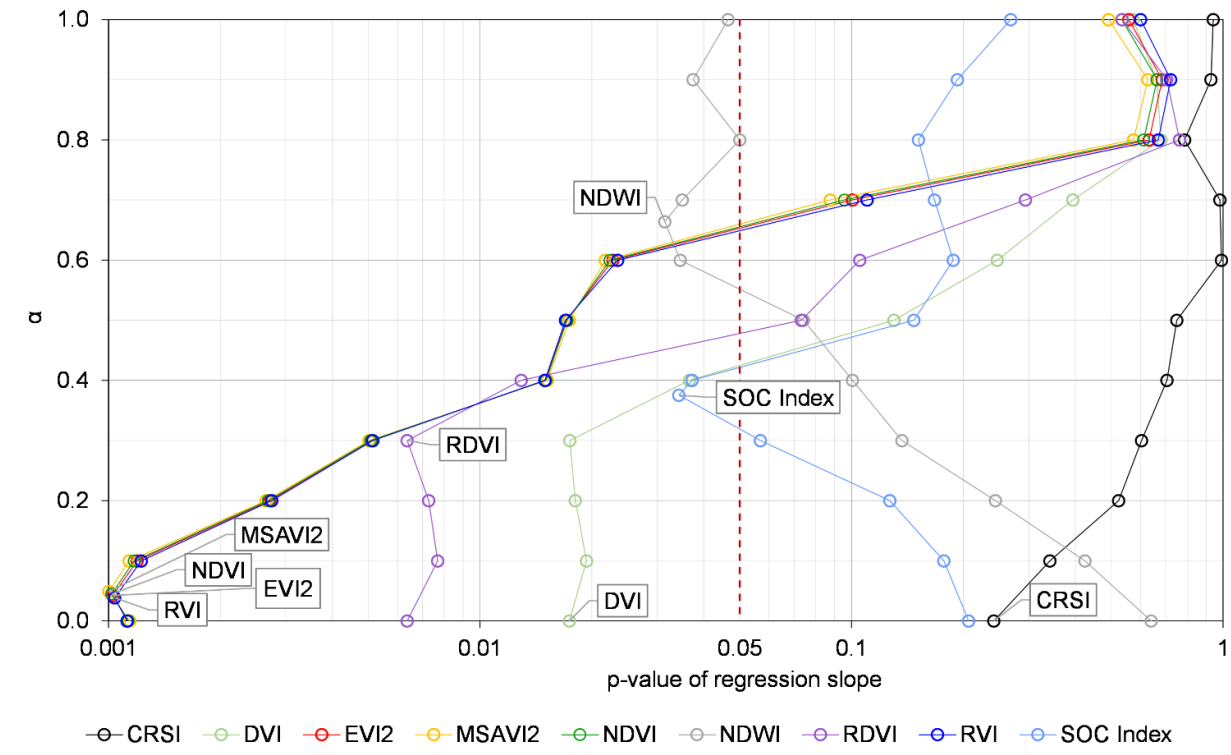

Fig. 3. P-value of the regression slope between topsoil SOC (2019 dataset) and different percentiles of multitemporal (α) Sentinel-2 spectral indices. The label indicates the optimal percentile for each spectral index. CRSI: Canopy Response Salinity Index, DVI: Difference Vegetation Index, EVI2: Enhanced Vegetation Index 2, MSAVI2: Modified Soil-Adjusted Vegetation Index 2, NDVI: Normalized Difference Vegetation Index, NDWI: Normalized Difference Water Index, RDVI: Renormalized Difference Vegetation Index, RVI: Ratio Vegetation Index, and SOC Index: Soil Organic Carbon Index.

Table 3 provides the regression statistics for the best-performing α for the EVI2, MSAVI2, NDVI, and RVI indices, which yielded very similar results. The four regression models had similar R^2 (~ 0.64) and RSME (~ 1.38) values. All the models were significant at the $p<0.01$ probability level. The four regression models also had very similar optimal α. The robustness of the percentile selection was tested using leave-one-out resampling. For EVI2, the LOO average α was 0.041 (standard deviation = 0.02561); for MSAVI2 it was 0.049 (standard deviation = 0.02571); for NDVI it was 0.044 (standard deviation = 0.02562); and for RVI it was 0.038 (standard deviation = 0.02557). The LOO analyses indicated that the optimal α values in Table 3 were fairly robust.

The selection of the 0.05 percentile (i.e., α = 0.05) NDVI is an approach used to distinguish bare-soil from vegetation by many authors (Jiang et al., 2010; Zeng et al., 2000; Montandon and Small, 2008; Ding et al., 2016). Our data-driven approach

indicated that α~0.05 is a good value to detect SOC on bare soil with NDVI and other spectral indices. Commonly, however, a threshold of NDVI = 0.25 (or other arbitrary value) is used to distinguish vegetation from bare soils in satellite images (Castaldi et al., 2019b; Demattê et al., 2018). The average (± standard deviation) values (across the two sites) corresponding to the α values in Table 3, were: for EVI, 0.14±0.03; for MSAVI, 0.17±0.03; for NDVI, 0.09±0.02 (which is remarkably lower than arbitrary thresholds selected in other research); and for RVI, 1.21±0.04.

Table 3
Regression statistics between topsoil SOC (2019 dataset) and the selected spectral indices. The α values indicate the percentile value for the multitemporal time series of the spectral indices.

Spectral index	*n*	α	R^2	Intercept (95% CI)	Slope (95% CI)	p-value
EVI2	13	0.042	0.640	34.368 (29.166, 39.569)	-72.334 (-108.348, -36.320)	0.001
MSAVI2	13	0.049	0.641	36.025 (30.029, 42.021)	-70.183 (-105.012, -35.354)	0.001
NDVI	13	0.045	0.640	34.854 (29.420, 40.288)	-115.792 (-173.378, - 58.206)	0.001
RVI	13	0.039	0.639	80.485 (52.346, 108.625)	-46.805 (-70.144, -23.465)	0.001

EVI2: Enhanced Vegetation Index 2, MSAVI2: Modified Soil-Adjusted Vegetation Index 2, NDVI: Normalized Difference Vegetation Index, RVI: Ratio Vegetation Index, *n* = number of sampling locations; R^2 = coefficient of determination; CI = confidence interval.

1.3.2 Terrain attributes

The elevation values ranged approximately from 627 to 699 m, and TWI from 10.0 to 17.5. The slope values varied from 0.1 to 20.3%, with a mean of 5.5%. According to the slope classes suggested by the Brazilian Agricultural Research Corporation (EMBRAPA, 1999). Most of the study area can be classified as a slightly wavy (3-8%) terrain, with the slope gradient varying from flat (0-3%) to wavy (8-20%).

Table 4 provides the statistics of the linear regression between the standardized topographic indicators and topsoil SOC (2019 dataset). The linear regression between

the standardized elevation and SOC had $R^2 = 0.70$ ($p<0.01$) and RSME = 1.26. On the contrary, the standardized slope and TWI were not good predictors for SOC.

Since the standardized elevation presented the best performance, it was selected as a proxy for topsoil SOC (2019) spatial variability in the study area. Generally, several evidences showed that SOC has a positive correlation with elevation (Tsozué et al., 2019; He et al., 2020), which is corroborated by the results of the present study. Wang et al. (2018a) collected topsoil (0-0.2 m) samples in a northeastern agroecosystem area of China to study the spatial distribution of SOC. They observed that elevation was the most important topographic variable to predict SOC. Zhou et al. (2020) collected topsoil (0-0.2 m) samples in a watershed located in northwestern China, to assess the use of multitemporal Sentinel-1A data in SOC estimation. They also concluded that elevation was the most important topographic variable for predicting SOC. Those findings are consistent with the results presented in this study, and highlight the relevance of elevation as a potential proxy for assessing the topsoil SOC.

Table 4
Regression statistics between topsoil SOC (2019 dataset) and the standardized topography indicators.

Standardized indicator	*n*	R^2	Intercept (95% CI)	Slope (95% CI)	p-value
Elevation	13	0.702	24.085 (23.249, 24.921)	2.011 (1.140, 2.881)	0.0004
Slope	13	0.191	24.085 (22.708, 25.462)	-1.048 (-2.482, 0,385)	0.136
TWI	13	0.021	24.085 (22.571, 25.599)	0.352 (-1.224, 1.928)	0.633

n = number of sampling locations; R^2 = coefficient of determination; CI = confidence interval; TWI = Topographic wetness index.

1.3.3 Sampling scheme comparison and topsoil SOC temporal changes

Figure 4 presents the maps of multitemporal NDVI using α=0.045 (Fig. 4a) and elevation (Fig. 4c). The whole-area values, those at the 2012-2016 sampling sites, and those at the 2019 sampling sites are compared in the boxplots of Figs. 4b (for the NDVI map) and 4d (for the elevation map). The NDVI average values were very close across the boxplots (0.096 considering all the pixels of the study area, 0.094 for the 2012-2016 sampling scheme, and 0.093 for the 2019 sampling scheme, respectively). Similarly, the average elevation at the two sites was = 670 m, which was very close to

that of 2012-2016 (671 m) and 2019 (669 m) sampling schemes. The ANOVA test indicated that the mean values across the three boxplots were non-significantly different for both NDVI and elevation. These results indicated that both the 2012-2016 and the 2019 sampling schemes were both representative of the whole-area frequency statistics for both NDVI and elevation. It should be noted that only the results for NDVI are reported here for the sake of conciseness, but EVI2, MSAVI2, and RVI had equivalent results for NDVI and elevation.

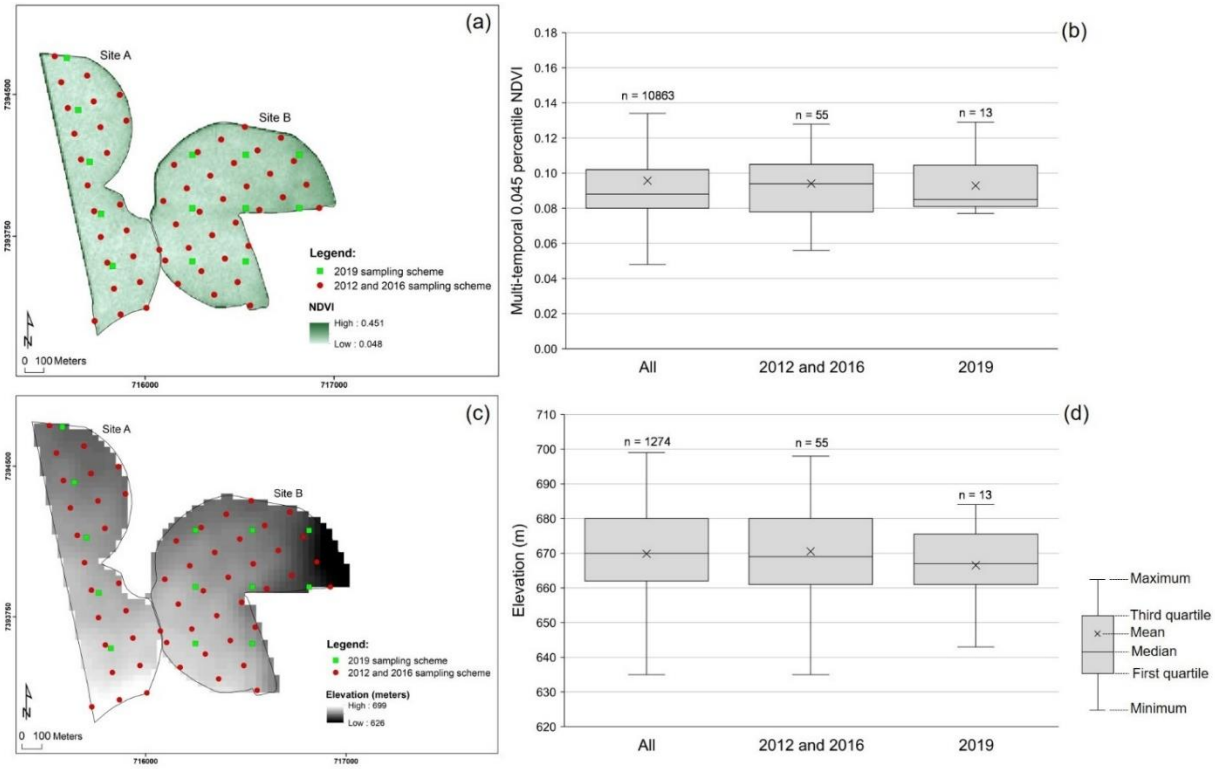

Fig. 4. Multitemporal 0.045 percentile of the Normalized Difference Vegetation Index (NDVI) map (a) and its frequency distribution (boxplots) for all the entire study area and the two different sampling schemes (b). Elevation map (c) and boxplots for the entire study area and the two different sampling schemes (d). Distribution outliers were not included in the boxplots.

Along the study years, at Site A, Figure 5(a) shows the topsoil SOC changes (mean of 22.53 and standard deviation of 3.01 in 2012; mean of 23.52 and standard deviation of 2.39 in 2016; and mean of 24.69 and standard deviation of 2.10 in 2019). The Wilcoxon test for paired samples (from 2012 to 2016) and the Kruskal-Wallis rank test (from 2016 to 2019) revealed no significant difference in the topsoil SOC at site A during the study period. Figure 5(b) shows the topsoil SOC changes (mean of 16.78 and standard deviation of 2.74 in 2012; mean of 24.90 and standard deviation of 2.56

in 2016; and mean of 23.71 and standard deviation of 2.63 in 2019) at site B. The Wilcoxon test for paired samples (from 2012 to 2016) presented a significant difference, and the Kruskal-Wallis rank test (from 2016 to 2019) showed no significant difference in the topsoil SOC at site B. Figure 5(c) shows the topsoil SOC changes (mean of 19.29 and standard deviation of 4.03 in 2012; mean of 24.30 and standard deviation of 2.56 in 2016; and mean of 24.08 and standard deviation of 2.40 in 2019) considering the sites together. The Wilcoxon test for paired samples (from 2012 to 2016) presented a significant difference, and the Kruskal-Wallis rank test (from 2016 to 2019) showed no significant difference in the topsoil SOC at the sites together. The mean SOC increased by 24.83% in the topsoil layer from 2012 to 2019.

1.3.4 Subsoil, whole profile, and SOC stratification ratio

Across the two sites, a linear regression described that the relationship between topsoil and subsoil SOC presented a poor statistical coupling in 2019 (slope = 0.57, intercept = 8.83, and R^2 = 0.26), and a better coupling in 2012 (slope = 0.69, intercept = 1.25, and R^2 = 0.74). Because of the lack of a strong correlation between soil layers, we could not infer if either of the sampling schemes were representative of the SOC distribution in the subsoil. Therefore, we did not perform any statistical test on the changes of subsoil SOC between 2012 and 2019.

Figure 5(d) shows the subsoil SOC changes (mean of 14.98 and standard deviation of 2.06 in 2012; and mean of 23.14 and standard deviation of 2.73 in 2019) at site A. Figure 5(e) shows the subsoil SOC changes (mean of 9.67 and a standard deviation of 1.64 in 2012; and mean of 22.30 and a standard deviation of 2.83 in 2019) at site B. Figure 5(f) shows the subsoil SOC changes (mean of 11.99 and standard deviation of 3.22 in 2012; and mean of 22.63 and standard deviation of 2.71 in 2019) at both the sites A and B considered together, which presented an increase of 88.74% in SOC occurred over the course of seven years.

Using a worldwide database from several published studies, West and Post (2002) reported that a significant increase in SOC occurred in the 0-0.07 and 0.07-0.15 m soil layers, while no significant increase in the 0.15-0.25 and 0.25-0.35 m layers when the tillage system was shifted from CT to NT. Additionally, the same authors reported that most of the sequestered carbon (~85%) was found in the first 0.07 m of soil depth. From another global analysis, Haddaway et al. (2017) observed that SOC content was

significantly higher under NT in the 0-0.15 m soil layer, compared to tillage systems. Also, the same authors reported that the intermediate intensity tillage (non-inversion tillage practice at 0-0.40 m soil layer) showed significantly higher SOC in 0-0.15 and 0.15-0.30 m compared to high-intensity tillage systems (inversion or non-inversion tillage practice at until or below 0.40 m depth). In an experiment conducted in a Brazilian oxisol, Sá et al. (2001) showed that 22 years of NT (with crop rotation) had significantly higher SOC content in 0-0.025 and 0.025-0.05 m compared to 22 years of CT. Whereas the CT showed higher SOC in the 0.20-0.40 m depth range and did not show a significant difference in 0.05-0.10 and 0.10-0.20 m. In the present study, the combination of reduced tillage together with crop rotation, use of crop residues, and irrigation showed an increase in SOC content in the 0-0.20 m and 0.20-0.40 m soil depth. Since many studies reported divergent results on SOC accumulation layers under agriculture management systems, Angers and Eriksen-Hamel (2008) emphasized the importance of considering the entire soil profile (0-0.40 m) for SOC comparations.

Figure 5(g) shows the SOC changes along the entire profile (mean of 18.75 and standard deviation of 2.34 in 2012; and mean of 23.92 and standard deviation of 1.95 in 2019) at site A. Figure 5(h) shows the SOC changes along the entire profile (mean of 13.23 and standard deviation of 2.01 in 2012; and mean of 23.01 and standard deviation of 2.43 in 2019) at site B. Figure 5(i) shows the SOC changes along the entire profile (mean of 15.64 and standard deviation of 3.50 in 2012; and mean of 23.36 and standard deviation of 2.22 in 2019) at both the sites considered together, showing an increase of 49.36% occurring over the course of seven years.

Figure 5(j) shows the SOC stratification ratio (ratio of topsoil SOC divided by the subsoil SOC) changes (mean of 1.51 and standard deviation of 0.16 in 2012; and mean of 1.08 and a standard deviation of 0.12 in 2019) at site A. Figure 5(k) shows the SOC stratification ratio changes (mean of 1.75 and standard deviation of 0.24 in 2012; and mean of 1.07 and a standard deviation of 0.12 in 2019) at site B. Figure 5(l) shows the SOC stratification ratio changes (mean of 1.65 and standard deviation of 0.24 in 2012; and mean of 1.07 and standard deviation of 0.11 in 2019) at both the sites A and B considered together.

Again, when considering both the sites A and B together, the mean SOC stratification ratio decreased by 35.15% from 2012 to 2019. This may be explained by the greater increase of SOC in the subsoil compared to the topsoil layer. Regardless

of the decrease in SOC content with depth, the subsoil is recognized as a potential carbon sink (Alcántara et al., 2017) as it presents higher SOC stability compared to the topsoil layer (Luo et al., 2019). It is possible to increase SOM through reduced tillage and root growth, as indicated by Moore et al. (2019). Dietzel et al. (2017) mentioned that the crop root system produces a significant contribution to the SOC pool. These authors concluded that corn could produce more carbon at deeper depths, whereas prairies can generate more carbon at superficial soil depths.

As it was not possible to confirm that the subsoil SOC sampling schemes are comparable, statistical tests were not used to analyze the changes in the subsoil, along the entire profile, and the stratification ratio.

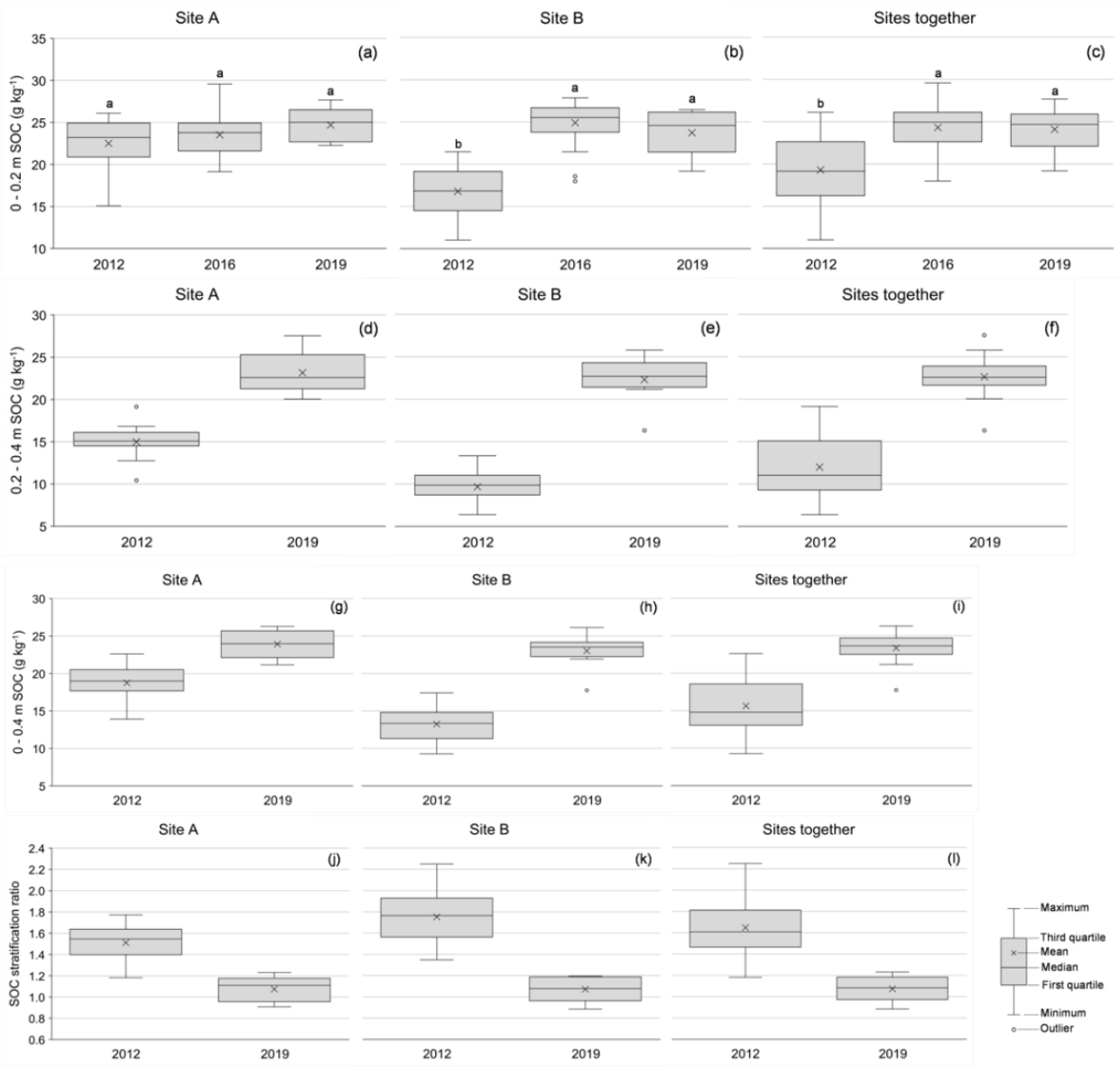

Fig. 5. SOC changes in the topsoil (0 – 0.2 m), subsoil (0.2 – 0.4 m), along the entire profile (0 – 0.4m), and stratification ratio (topsoil/subsoil) at the study area over the course of the study years, considering the sites A and B individually and together.

1.4 CONCLUSIONS

The results from the research study presented in this article demonstrate that the multitemporal dataset obtained Sentinel-2 can be used to derive the most suitable spectral indices to estimate the topsoil SOC content in the study area. The use of the multitemporal imagery enabled to achieve higher accuracy in estimating the topsoil SOC relative to that obtained from the use of single-date images, as the relationship between topsoil SOC and spectral indices varied with the acquisition date of Sentinel-2 images. Within the tested spectral indices, EVI2, MSAVI2, NDVI, and RVI provided the best correlations with SOC, which were very similar. Considering the indicated related to the topography, the elevation offered a significant correlation gain.

NDVI and elevation were selected as the best spatial covariates in the study area. Their frequency distribution indicated that the two different SOC sampling schemes were representative of the study area. By investigating changes that occurred over the course of seven years, we observed a significant increase in the topsoil SOC. However, it was not possible to make inferences about the subsoil SOC from the topsoil SOC (2019 dataset), because its relationship showed a poor statistical coupling.

The present study identified remotely sensed proxies to assess SOC across a field scale, which can be readily used by the farming community, land managers, agriculture consultants, and policy makers. The results also allowed clarifying that a few years of conservation practices can promote significant effects on the increase of SOC content.

Future research should investigate the relationship between remote sensing data and topsoil SOC for areas characterized by soil variability, using remote sensing data with higher spatial resolution, and assess the time necessary to reverse the SOC gains resulting from conservation practices. Finally, future studies should also explore the relationship between SOC and the amount of water applied through the irrigation system.

Declaration of Competing Interest

The authors declare that there is no conflict of interest regarding the publication of this article.

Acknowledgments

The authors wish to acknowledge the National Council for Scientific and Technological Development (CNPq) for granting a scholarship (grant number: 140676/2017-1) to the first author. Additionally, the authors acknowledge the Institutional Program for Internationalization of Higher Education Institutions and Research Institutions (PrInt) by the Brazilian Federal Agency for Support and Evaluation of Graduate Education (CAPES) for the financial support (grant number: 88887.364471/2019-00) for a research period at the University of California, Davis, to the first author. The authors thank Abel Rodrigues Simões Junior from “Olhos D’Água” farm for the support and for providing the results from soil analysis.

Supplementary data

Table S1

5-year crop rotation at each study site.

Location	Crop	Date of sowing	Date of harvest
Site A	Corn	January 21, 2014	July 03, 2014
	Bean	August 20, 2014	December 04, 2014
	Corn	December 16, 2014	May 21, 2015
	Bean	June 23, 2015	October 14, 2015
	Cotton	October 15, 2015	May 07, 2016
	Corn	August 28, 2016	February 09, 2017
	Corn	February 14, 2017	July 30, 2017
	Bean	August 23, 2017	December 14, 2017
	Potato	The land was leased	
	Soybean	September 12, 2018	January 06, 2019
	Bean	January 07, 2019	April 22, 2019
Site B	Corn	December 26, 2013	May 30, 2014
	Bean	August 18, 2014	December 02, 2014
	Soybean	December 09, 2014	April 06, 2015
	Bean	July 18, 2015	November 11, 2015
	Cotton	November 12, 2015	June 10, 2016
	Bean	September 13, 2016	December 18, 2016
	Corn	January 03, 2017	July 07, 2017
	Bean	August 28, 2017	December 14, 2017
	Corn	January 06, 2018	July 08, 2018
	Bean	July 09, 2018	October 25, 2018
	Cotton	December 05, 2018	April 22, 2019

REFERENCES

Alcántara, V., Don, A., Vesterdal, L., Well, R., Nieder, R., 2017. Stability of buried carbon in deep-ploughed forest and cropland soils - implications for carbon stocks. Sci. Rep. 7, 5511. doi:10.1038/s41598-017-05501-y

Angelopoulou, T., Balafoutis, A., Zalidis, G., Bochtis, D., 2020. From laboratory to proximal sensing spectroscopy for soil organic carbon estimation—A review. Sustainability 12, 443. doi:10.3390/su12020443

Angelopoulou, T., Tziolas, N., Balafoutis, A., Zalidis, G., Bochtis, D., 2019. Remote sensing techniques for soil organic carbon estimation: A review. Remote Sens. 11, 676. doi:10.3390/rs11060676

Angers, D.A., Eriksen-Hamel, N.S., 2008. Full-inversion tillage and organic carbon distribution in soil profiles: A meta-analysis. Soil Sci. Soc. Am. J. 72 (5), 1370-1374. doi:10.2136/sssaj2007.0342

Batjes, N.H., 1996. Total carbon and nitrogen in the soils of world. Eur. J. Soil Sci. 47, 151-163. doi: https://doi.org/10.1111/j.1365-2389.1996.tb01386.x

Ben-Dor, E., Inbar, Y., Chen, Y., 1997. The reflectance spectra of organic matter in the visible near-infrared and short wave infrared region (400–2500 nm) during a controlled decomposition process. Remote Sens. Environ. 61, 1–15. doi:http://doi.org/10.1016/S0034-4257(96)00120-4.

Castaldi, F., Chabrillat, S., Don, A., Van Wesemael, B., 2019a. Soil organic carbon mapping using LUCAS topsoil database and Sentinel-2 data: An approach to reduce soil moisture and crop residue effects. Remote Sens. 11, 2121. doi:10.3390/rs11182121.

Castaldi, F., Huenib, A., Chabrillatc, S., Wardc, K., Buttafuocod, G., Bomanse, B., Vreyse, K., Brellc, M., Van Wesemaela, B., 2019b. Evaluating the capability of the Sentinel 2 data for soil organic carbon prediction in croplands. ISPRS J. Photogramm. Remote Sens. 147, 267–282. doi:https://doi.org/10.1016/j.isprsjprs.2018.11.026.

Castaldi, F., Palombo, A., Santini, F., Pascucci, S., Pignatti, S., Casa, R., 2016. Evaluation of the potential of the current and forthcoming multispectral and hyperspectral imagers to estimate soil texture and organic carbon. Remote Sens. Environ. 179, 54‑65. doi:http://dx.doi.org/10.1016/j.rse.2016.03.025.

Chen, Y., Li, Y., Wang, X., Wang, J., Gong, X., Niu, Y., Liu, J., 2020. Estimating soil organic carbon density in Northern China's agro-pastoral ecotone using vis-NIR spectroscopy. J. Soils Sediments. doi:https://doi.org/10.1007/s11368-020-02668-2.

CIIAGRO. Centro Integrado de Informações Agrometeorológicas. http://www.ciiagro.sp.gov.br/ (accessed 20 October 2020).

Claassen, R., Bowman, M., McFadden, J., Smith, D., Wallander, S., 2018. Tillage intensity and conservation cropping in the United States, EIB-197, U.S. Department of Agriculture, Economic Research Service.

Demattê, J.A.M., Fongaro, C.T., Rizzo, R., Safanelli, J.L., 2018. Geospatial Soil Sensing System (GEOS3): A powerful data mining procedure to retrieve soil spectral reflectance from satellite images. Remote Sens. Environ. 212, 161–175. doi:https://doi.org/10.1016/j.rse.2018.04.047.

Dietzel, R., Liebman, M., Archontoulis, S., 2017. A deeper look at the relationship between root carbon pools and the vertical distribution of the soil carbon pool. Soil 3, 139–152. doi:https://doi.org/10.5194/soil-3-139-2017.

Ding, Y., Zheng, X., Zhao, K., Xin, X., Liu, H., 2016. Quantifying the impact of $NDVI_{soil}$ determination methods and $NDVI_{soil}$ variability on the estimation of fractional vegetation cover in Northeast China. Remote Sens. 8, 29. doi:10.3390/rs8010029.

EMBRAPA. Empresa Brasileira de Pesquisa Agropecuária, 1999. Sistema brasileiro de classificação de solos. Brasília, Serviço de Produção de Informação.

Eskandari, I., Navid, H., Rangzan, K., 2016. Evaluating spectral indices for determining conservation and conventional tillage systems in a vetch-wheat rotation. Int. Soil Water Cons. Res. 4, 93-98. doi:https://doi.org/10.1016/j.iswcr.2016.04.002.

European Space Agency, 2015. Sentinel-2 user handbook. In: ESA Standard Document.

Fathololoumi, S., Vaezi, A.R., Alavipanah, S.K., Ghorbani, A., Saurette, D., Biswas, A., 2020. Improved digital soil mapping with multitemporal remotely sensed satellite data fusion: A case study in Iran. Sci. Total Environ. 721, 137703. doi:https://doi.org/10.1016/j.scitotenv.2020.137703.

Ferreira, A.V., Sánchez-Román, R.M., Orellana González, A.M.G., 2016. Temporal dynamic modeling for the assessment of water availability and its effects on sustainability of water resources at Boi Branco sub-basin, SP, Brazil. Athens J. Sci. 3 (2), 137-154. doi:https://doi.org/10.30958/ajs.3-2-4.

Gao, B., 1996. NDWI—A normalized difference water index for remote sensing of vegetation liquid water from space. Remote Sens. Environ. 58 (3), 257-266. doi:https://doi.org/10.1016/S0034-4257(96)00067-3.

Gholizadeh, A., Žižala, D., Saberioon, M., Borůvka, L., 2018. Soil organic carbon and texture retrieving and mapping using proximal, airborne and Sentinel-2 spectral imaging. Remote Sens. Environ. 218, 89-103. doi:https://doi.org/10.1016/j.rse.2018.09.015.

Grinand, C., Maire, G.L., Vieilledent, G., Razakamanarivo, H., Razafimbelo, T., Bernoux, M., 2017. Estimating temporal changes in soil carbon stocks at ecoregional scale in Madagascar using remote-sensing. Int. J. Appl. Earth Obs. Geoinf. 54, 1–14. doi:https://doi.org/10.1016/j.jag.2016.09.002.

Google Earth Version 9.124.0.1 (June 19, 2019). Itaí (SP), Brazil. 23º33'07"S, 48º53'00"W, altitude: 680 m, camera: 3,268. Maxar Technologies 2020. https://www.google.com/earth/ (accessed 01 October 2020).

Haddaway, N.R., Hedlund, K., Jackson, L.E., Kätterer, T., Lugato, E., Thomsen, I.K., Jørgensen, H.B., Isberg, P., 2017. How does tillage intensity affect soil organic carbon? A systematic review. Environ. Evid. 6, 30. doi:10.1186/s13750-017-0108-9.

He, G., Zhang, Z., Zhang, J., Huang, X., 2020. Soil organic carbon dynamics and driving factors in typical cultivated land on the Karst Plateau. Int. J. Environ. Res. Public Health 17, 5697. doi:https://doi.org/10.3390/ijerph17165697.

Heaton, L., Fullen, M.A., Bhattacharyya, R., 2016. Critical analysis of the van Bemmelen conversion factor used to convert soil organic matter data to soil organic carbon data: Comparative analyses in a UK loamy sand soil. Espaço Aberto 6 (1), 35-44. doi: https://doi.org/10.36403/espacoaberto.2016.5244.

Huang, J., Hartemink, A.E., Zhang, Y., 2019. Climate and land-use change effects on soil carbon stocks over 150 years in Wisconsin, USA. Remote Sens. 11 (12), 1504. doi:https://doi.org/10.3390/rs11121504.

Huynh, H.T., Hufnagel, J., Wurbs, A., Bellingrath-Kimura, S.D., 2019. Influences of soil tillage, irrigation and crop rotation on maize biomass yield in a 9-year field study in Müncheberg, Germany. Field Crops Res. 241, 1075652. doi:https://doi.org/10.1016/j.fcr.2019.107565.

IUSS Working Group WRB, 2015. World reference base for soil resources 2014, update 2015: International soil classification system for naming soils and creating legends for soil maps. World Soil Resources Reports No. 106. FAO, Rome. http://www.fao.org/soils-portal/soil-survey/soil-classification/ world-reference-base/en/ (accessed 20 October 2020).

Jensen, J.R., 2007. Remote sensing of the environment: An earth resource perspective, 2nd ed., Upper Saddle River, NJ: Prentice Hall.

Jiang, Z., Huete, A.R., Didan, K., Miura, T., 2008. Development of a two-band enhanced vegetation index without a blue band. Remote Sens. Environ. 112 (10), 3833-3845. doi:https://doi.org/10.1016/j.rse.2008.06.006.

Jiang, L., Kogan, F.N., Guo, W., Tarpley, J.D., Mitchell, K.E., Ek, M.B., Tian, Y., Zheng, W., Zou, C., Ramsay, B.H., 2010. Real-time weekly global green vegetation fraction derived from advanced very high resolution radiometer-based NOAA operational global vegetation index (GVI) system. J. Geophys. Res. 115, D11114 doi:10.1029/2009JD013204.

Kumar,P., Sajjad, H., Tripathy, B.R., Ahmed, R., Mandal, V.P., 2017. Prediction of spatial soil organic carbon distribution using Sentinel-2A and field inventory data in Sariska Tiger Reserve. Nat. Hazards. doi:10.1007/s11069-017-3062-5.

Kumar, N., Velmurugan, A., Hamm, N.A.S., Dadhwal, V.K., 2018. Geospatial mapping of soil organic carbon using regression kriging and remote sensing. J. Indian Soc. Remote Sens. doi:https://doi.org/10.1007/s12524-017-0738-y.

Kunkel, V., Hancock, G.R., Wells, T., 2019. Large catchment-scale spatiotemporal distribution of soil organic carbon. Geoderma 334, 175–185. doi:https://doi.org/10.1016/j.geoderma.2018.07.046.

Lal, R., 2004. Agricultural activities and the global carbon cycle. Nutr. Cycl. Agroecosystems 70, 103–116. doi: https://doi.org/10.1023/B:FRES.0000048480.24274.0f.

Lal, R., 2018. Digging deeper: A holistic perspective of factors affecting soil organic carbon sequestration in agroecosystems. Glob. Change Biol. 24, 3285–3301. doi:https://doi.org/10.1111/gcb.14054.

Landau, E.C., Guimarães, D.P., Silva, P.A.A., Souza, D.L., 2014. Concentração de áreas irrigadas por pivôs centrais no Estado de São Paulo - Brasil. Boletim de pesquisa e desenvolvimento n. 100. Sete Lagoas: Embrapa Milho e Sorgo.

Li, Y., Li, Z., Chang, S.X., Cui, S., Jagadamma, S., Zhang, Q., Cai, Y., 2020. Residue retention promotes soil carbon accumulation in minimum tillage systems: Implications for conservation agriculture, Sci. Total Environ. 740, 140147. doi:https://doi.org/10.1016/j.scitotenv.2020.140147.

Liang, Z., Chen, S. Yang, Y., Zhou, Y., Shi, Z., 2019. High-resolution three-dimensional mapping of soil organic carbon in China: Effects of Soil Grids products on national modeling. Sci. Total Environ. 685, 480–489. doi:https://doi.org/10.1016/j.scitotenv.2019.05.332.

Liu, M., Wang, T., Skidmore, A.K., Liu, X., 2018. Heavy metal-induced stress in rice crops detected using multi-temporal Sentinel-2 satellite images. Science of the Total Environment 637–638, 18–29. doi:https://doi.org/10.1016/j.scitotenv.2018.04.415.

Luo, Z., Wang, G., Wang, E., 2019. Global subsoil organic carbon turnover times dominantly controlled by soil properties rather than climate. Nat. Commun. 10, 3688. doi:https://doi.org/10.1038/s41467-019-11597-9.

Mattivi, P., Franci, F., Lambertini, A., Bitelli, G., 2019. TWI computation: a comparison of different open source GISs. Open Geospatial Data, Softw. Stand. 4, 6. doi:https://doi.org/10.1186/s40965-019-0066-y.

Mirchooli, F., Kiani-Harchegani, M., Darvishan, A.K., Falahatkar, S., Sadeghi, S.H., 2020. Spatial distribution dependency of soil organic carbon content to important environmental variables. Ecol. Indic. 116, 106473. doi:https://doi.org/10.1016/j.ecolind.2020.106473.

Mishra, U., Lal, R., Liu, D., Van Meirvenne, M., 2010. Predicting the spatial variation of the soil organic carbon pool at a regional scale. Soil Sci. Soc. Am. J. 74, 906‑914. doi:10.2136/sssaj2009.0158.

Montandon, L.M., Small, E.E., 2008. The impact of soil reflectance on the quantification of the green vegetation fraction from NDVI. Remote Sens. Environ. 112, 1835–1845. doi:10.1016/j.rse.2007.09.007.

Moore, I.D., Gessler, P.E., Nielsen, G.A., Peterson, G.A., 1993. Soil attribute prediction using terrain analysis. Soil Sci. Soc. Am. J. 57 (2), 443–452.

Moore, K.J., Anex, R.P., Elobeid, A.E., Fei, S., Flora, C.B., Goggi, A.S., Jacobs, K.L., Jha, P., Kaleita, A.L., Karlen, D.L., Laird, D.A., Lenssen, A.W., Lübberstedt, T., McDaniel, M.D., Raman, D.R., Weyers, S.L., 2019. Regenerating agricultural landscapes with perennial groundcover for intensive crop production. Agronomy 9, 458. doi:10.3390/agronomy9080458.

Norris, C.E., Katelyn A., Congreves, K.A., 2018. Alternative management practices improve soil health indices in intensive vegetable cropping systems: A review. Front. Environ. Sci. 6, 50. doi: 10.3389/fenvs.2018.00050.

Padilha, M.C.C., Vicente, L.E., Demattê, J.A.M., Loebmann, D.G.S.W., Vicente, A.K. Salazar, D.F.U., Guimarães, C.C.B., 2020. Using Landsat and soil clay content to map soil organic carbon of oxisols and Ultisols near São Paulo, Brazil. Geoderma Reg. 21, e00253. doi:https://doi.org/10.1016/j.geodrs.2020.e00253.

Paustian, K., Lehmann, J., Ogle, S., Reay, D., Robertson, G.P., Smith, P., 2016. Climate-smart soils. Nature 532, 49-57. doi:https://doi.org/10.1038/nature17174.

Pearlshtien, D.H., Ben-Dor, E., 2020. Effect of organic matter content on the spectral signature of iron oxides across the VIS–NIR spectral region in artificial mixtures: An example from a red soil from Israel. Remote Sens. 12, 1960. doi:10.3390/rs12121960.

Perry, C., Steduto, P., Allen, R.G., Burt, C.M., 2009. Increasing productivity in irrigated agriculture: Agronomic constraints and hydrological realities. Agric. Water Manag. 96, 1517–1524. doi:10.1016/j.agwat.2009.05.005.

Qi, J., Kerr, Y., Chehbouni, A., 1994. External factor consideration in vegetation index development. In: Proceeding of International Symposium on Physical Measurements and Signatures in Remote Sensing. Val D'Isere, France.

R Core Team, 2020. R: A language and environment for statistical computing. R Foundation for Statistical Computing, Vienna, Austria.

Rondeaux, G., Steven, M., Baret, F., 1996. Optimization of soil-adjusted vegetation indices. Remote Sens. Environ. 55 (2), 95–107. doi:https://doi.org/10.1016/0034-4257(95)00186-7.

Roujean, J.L., Breon, F.M., 1995. Estimating PAR absorbed by vegetation from bidirectional reflectance measurements. Remote Sens. Environ. 51 (3), 375−384. doi:https://doi.org/10.1016/0034-4257(94)00114-3.

Rouse, J.W., Haas, J.R.H., Schell, J.A., Deering, D.W., 1974. Monitoring vegetation systems
in the Great Plains with ERTS. In: Proceedings of the 3rd ERTS Symposium. Washington, USA.

Sá, J.C.M., Cerri, C.C., Dick, W.A., Lal, R., Venske Filho, S.P., Piccolo, M.C., Feigl, B.E., 2001. Organic matter dynamics and carbon sequestration rates for a tillage chronosequence in a Brazilian Oxisol. Soil Sci. Soc. Am. J. 65, 1486–1499. doi: https://doi.org/10.2136/sssaj2001.6551486x.

Santos, F., Ramalho, L.S., Marques, T.A., Sena-Souza, J.P., Reatto, A., Martins, E.S., Couto Jr, A.F., Nardoto, G.B., 2014. Teor de carbono orgânico do solo e aspectos biofísicos da cobertura vegetal da bacia do Córrego Sarandi, Planaltina, DF. Embrapa Cerrados.

Scudiero, E., Skaggs, T.H., Corwin, D.L., 2014. Regional scale soil salinity evaluation using Landsat 7, western San Joaquin Valley, California, USA. Geoderma Reg. 2–3, 82–90. doi:http://dx.doi.org/10.1016/j.geodrs.2014.10.004.

Scudiero, E., Skaggs, T.H., Corwin, D.L., 2015. Regional-scale soil salinity assessment using Landsat ETM+ canopy reflectance. Remote Sens. Environ. 169, 335–343. doi:http://dx.doi.org/10.1016/j.rse.2015.08.026.

Scudiero, E., Teatini, P., Manoli, G., Braga, F., Skaggs, T.H., Morari, F., 2018. Workflow to establish time-specific zones in precision agriculture by spatiotemporal integration of plant and soil sensing data. Agronomy 8, 253. doi:10.3390/agronomy8110253.

Sena, N.C., Veloso, G.V., Fernandes-Filho, E.I., Marcelino. M.R., Schaefer, C.E.G.R., 2020. Analysis of terrain attributes in different spatial resolutions for digital soil mapping application in southeastern Brazil. Geoderma Reg. 21, e00268.. doi:https://doi.org/10.1016/j.geodrs.2020.e00268.

SiBCS. Sistema Brasileiro de Classificação de Solos, 2018. Fifth ed. Brasília, DF: EMBRAPA Solos.

Souza, J.V.R.S., Saad, J.C.C., Sánchez-Román, R.M., Rodríguez-Sinobas, L., 2016. No-till and direct seeding agriculture in irrigated bean: Effect of incorporation crop residues on soil water availability and retention, and yield. Agric. Water Manag. 170, 158-166. doi:https://doi.org/10.1016/j.agwat.2016.01.002.

Tautges, N.E., Chiartas, J.L., Gaudin, A.C.M., O'green, A.T., Herrera, I., Scow, K.M., 2019. Deep soil inventories reveal that impacts of cover crops and compost on soil carbon sequestration differ in surface and subsurface soils. Glob. Chang. Biol. 25, 3753–3766. doi:https://doi.org/10.1111/gcb.14762.

Thaler, E.A.; Larsen, I.J.; Yu, Q., 2019. A new index for remote sensing of soil organic carbon based solely on visible wavelengths. Soil Sci. Soc. Am. J. 83, 1443–1450. doi:10.2136/sssaj2018.09.0318.

Thomsen, L.M., Baartman, J.E.M., Barneveld, R.J., Starkloff, T., Stolte, J., 2015. Soil surface roughness: comparing old and new measuring methods and application in a soil erosion model. Soil 1, 399–410. doi:10.5194/soil-1-399-2015.

Trost, B., Prochnow, A., Drastig, K., Meyer-Aurich, A., Ellmer, F., Baumecker, M., 2013. Irrigation, soil organic carbon and N_2O emissions. A review. Agron. Sustain. Dev. 33, 733–749. doi:https://doi.org/10.1007/s13593-013-0134-0.

Tsozué, D., Nghonda, J.P., Tematio, P., Basga, S.D., 2019. Changes in soil properties and soil organic carbon stocks along an elevation gradient at Mount Bambouto, Central Africa. Catena 175, 251–262. doi:https://doi.org/10.1016/j.catena.2018.12.028.

Tucker C., 1979. Red and photographic infrared linear combinations for monitoring vegetation. Remote Sens. Environ. 8 (2),127–150. doi:https://doi.org/10.1016/0034-4257(79)90013-0.

Valeriano, M.M., Rossetti, D.F., 2012. Topodata: Brazilian full coverage refinement of SRTM data. Appl. Geogr. 32, 300–309. doi:https://doi.org/10.1016/j.apgeog.2011.05.004.

Vaudour, E., Gomez, C., Loiseau, T, Baghdadi, N., Loubet, B., Arrouays, D., Ali, L., Lagacherie, P., 2019. The impact of acquisition date on the prediction performance of topsoil organic carbon from Sentinel-2 for croplands. Remote Sens. 11, 2143. doi:10.3390/rs11182143.

Walkley, A., Black, I.A., 1934. An examination of the Degtjareff method for determining soil organic matter, and proposed modification of the chromic acid titration method. Soil Sci. 37 (1), 29-38. doi:10.1097/00010694-193401000-00003.

Wang, S., Adhikari, K., Wang, Q., Jin, X., Li, H., 2018a. Role of environmental variables in the spatial distribution of soil carbon (C), nitrogen (N), and C:N ratio from the northeastern coastal agroecosystems in China. Ecol. Indic. 84, 263–272. doi:http://dx.doi.org/10.1016/j.ecolind.2017.08.046.

Wang, X., Yoo, K., Wackett, A.A., Gutknecht, J., Amundson, R., Heimsath, A., 2018b. Soil organic carbon and mineral interactions on climatically different hillslopes. Geoderma 322, 71-80. doi:https://doi.org/10.1016/j.geoderma.2018.02.021.

Wang, X., Zhang, Y., Atkinson, P.M., Yao, H., 2020. Predicting soil organic carbon content in Spain by combining Landsat TM and ALOS PALSAR images. Int. J. Appl. Earth. Obs. Geoinf. 92, 102182. doi:https://doi.org/10.1016/j.jag.2020.102182.

West, T.O.; Post, W.M., 2002. Soil organic carbon sequestration rates by tillage and crop rotation: a global data analysis. Soil Sci. Soc. Am. J. 66, 1930. doi:http://dx.doi.org/10. 2136/sssaj2002.1930.

Xu, Y., Smith, S.E., Grunwald, S., Abd-Elrahman, A., Wani, S.P., Nair, V.D., 2018. Estimating soil total nitrogen in smallholder farm settings using remote sensing spectral

indices and regression kriging. Catena 163, 111–122. doi:https://doi.org/10.1016/j.catena.2017.12.011.

Xu, Y., Smith, S.E., Grunwald, S., Abd-Elrahman, A., Wani, S.P., 2017. Incorporation of satellite remote sensing pan-sharpened imagery into digital soil prediction and mapping models to characterize soil property variability in small agricultural fields. ISPRS J. Photogramm. Remote Sens. 123, 1–19. doi:https://doi.org/10.1016/j.isprsjprs.2016.11.001.

Xue, J., Su, B., 2017. Significant remote sensing vegetation indices: A review of developments and applications. J. Sens. article ID 1353691. doi:https://doi.org/10.1155/2017/1353691.

Yigini, Y., Olmedo, G.F., Reiter, S., Baritz, R., Viatkin, K. Vargas, R. (Eds.), 2018. Soil Organic Carbon Mapping Cookbook 2nd edition. Rome, FAO.

Ymeti, I., Pikha Shrestha, D., van der Meer, F., 2019. Monitoring soil surface mineralogy at different moisture conditions using visible near-infrared spectroscopy data. Remote Sens. 11, 2526. doi:https://doi.org/10.3390/rs11212526.

Zeng, X.B., Dickinson, R.E., Walker, A., Shaikh, M., DeFries, R.S., Qi, J.G., 2000. Derivation and evaluation of global 1-km fractional vegetation cover data for land modeling. J. Appl. Meteorol. 39, 826–839. doi:10.1175/1520-0450(2000)039<0826:daeogk>2.0.co;2.

Zhang, Y., Long, G., Chen, Y., Shi, T., Luo, M., Ju, Q., Zhang, H., Wang, S., 2019. Prediction of soil organic carbon based on Landsat 8 monthly NDVI data for the Jianghan Plain in Hubei Province, China. Remote Sens. 11, 1683. doi:10.3390/rs11141683.

Zhou, T., Geng, Y., Chen, J., Liu, M., Haase, D., Lausch, A., 2020. Mapping soil organic carbon content using multi-source remote sensing variables in the Heihe River Basin in China. Ecol. Indic. 114, 106288. doi:https://doi.org/10.1016/j.ecolind.2020.106288.

Žížala, D., Minařík, R., Zádorová, T., 2019. Soil Organic Carbon Mapping Using Multispectral Remote Sensing Data: Prediction Ability of Data with Different Spatial and Spectral Resolutions. Remote Sens. 11, 2947. doi:10.3390/rs11242947.

Zomer, R.J., Bossio, D.A., Sommer, R., Verchot, L.V., 2017. Global sequestration potential of increased organic carbon in cropland soils. Sci. Rep. 7, 15554. doi:10.1038/s41598-017-15794-8.

CHAPTER 2
MULTI-SCALE VARIABILITY OF SOIL ORGANIC CARBON AND TOTAL NITROGEN IN MATURE MICRO-IRRIGATED CITRUS ORCHARDS IN CALIFORNIA'S SAN JOAQUIN VALLEY

ABSTRACT: The spatial variability of soil organic carbon (SOC) and soil total nitrogen (STN) influences physicochemical and biological soil properties, enhancing water retention, soil aggregation, the reservoir of plant nutrients, and biodiversity. The determination of SOC and STN levels are important for sustainable agricultural management, by their influence on soil fertility, soil health, agricultural productivity, and food security. In the present research, a multi-scale spatial distribution of SOC and STN in citrus orchards was studied, to investigate the representativeness of tree-scale, along transects, relative to orchard-scale. Two mature micro-irrigated citrus orchards in California's San Joaquin Valley were selected, one with Page mandarin (*Citrus reticulata*) in Strathmore, and another with Washington navel orange (*Citrus sinensis*) in Ivanhoe. Both orchards are irrigated with micro-sprinklers, and the pruning residues are disposed on the inter-rows. The soil was sampled along transects, and it was divided into three sections: section α located at 0.6 m from the tree trunk, section β at 1.2 m from the trunk (approximately below the canopy projection), and section γ located in the middle of the inter-row. In each section single samples were collected at two depths, from 0 to 0.05 m and from 0.05 to 0.4 m. A total of 20 transects were performed at the orchard in Strathmore, characterized by the presence of three soil groups, and six in Ivanhoe, which has one soil group. Additionally to the soil samples, plant tissue was collected for plant total carbon (PTC) and plant total nitrogen (PTN) analysis. In Ivanhoe, where there is a more homogeneous soil, no significant differences were found between the sections and the orchard at the studied soil layers. In Strathmore, the first five centimeters soil layer showed higher mean levels of SOC and STN at section β, whereas from 0.05 to 0.40 m, the higher mean levels of SOC and STN were found at section α. From 0 to 0.05 m the mean values of SOC at sections β and γ and STN at section γ were not statistically different from the mean value of the whole orchard. From 0.05 to 0.40 m and from 0 to 0.40 m there was no statistical difference between the sections and the orchard. Considering the three soil groups in Strathmore, significant statistical differences were found only in the top five centimeters of the soil, and no differences were found in the mean values of PTC and PTN along

with the soil groups. The present research provides support for future soil sampling procedures, projects on SOC and STN monitoring, and agricultural management in the study area.

Keywords: Micro-sprinkler irrigation. Pruning residue. San Joaquin Valley. Soil health. Tulare county.

RESUMO: A variabilidade espacial do carbono orgânico do solo (COS) e do nitrogênio total do solo (NTS) influencia as propriedades físico-químicas e biológicas do solo, aumentando a retenção de água, a agregação do solo, o reservatório de nutrientes para as plantas e a biodiversidade. A determinação dos níveis de SOC e STN são importantes para o manejo agrícola sustentável, por sua influência na fertilidade do solo, saúde do solo, produtividade agrícola e segurança alimentar. Na presente pesquisa, uma distribuição espacial multi-escala de COS e NTS em pomares de citros foi estudada, para investigar a representatividade da escala de árvore, ao longo de transectos, em relação à escala de pomar. Dois pomares cítricos micro-irrigados em San Joaquin Valley na Califórnia foram selecionados, um com *Page mandarin* (*Citrus reticulata*) em Strathmore, e outro com *Washington navel orange* (*Citrus sinensis*) em Ivanhoe. Ambos os pomares são irrigados com microaspersores, e os resíduos da poda são dispostos nas entrelinhas. O solo foi amostrado ao longo de transectos e dividido em três seções: seção α localizada a 0,6 m do tronco da árvore, seção β a 1,2 m do tronco (aproximadamente abaixo da projeção da copa) e seção γ localizada no centro da entrelinha. Em cada seção, amostras individuais foram coletadas em duas profundidades, de 0 a 0,05 m e de 0,05 a 0,4 m. Um total de 20 transectos foi realizado no pomar em Strathmore, caracterizado pela presença de três grupos de solos, e seis em Ivanhoe, que possui um grupo de solo. Além das amostras de solo, material vegetal foi coletado para análise do carbono total da planta (CTP) e do nitrogênio total da planta (NTP). Em Ivanhoe, onde existe um solo mais homogêneo, não foram encontradas diferenças significativas entre as seções e o pomar nas camadas de solo estudadas. Em Strathmore, a primeira camada de cinco centímetros de solo apresentou maiores níveis médios de COS e NTS na seção β, enquanto de 0,05 a 0,40 m, os maiores níveis médios de COS e NTS foram encontrados na seção α. De 0 a 0,05 m, os valores médios de COS nas seções β e γ e NTS na seção γ não foram estatisticamente diferentes do valor médio de todo o pomar. De 0,05 a 0,40 m

e de 0 a 0,40 m não houve diferença estatística entre os transectos e o pomar. Considerando os três grupos de solo em Strathmore, diferenças estatísticas significativas foram encontradas apenas nos cinco centímetros superiores do solo, e nenhuma diferença foi encontrada nos valores médios de CTP e NTP entre os grupos de solo. A presente pesquisa fornece suporte para procedimentos futuros de amostragem de solo, projetos de monitoramento de COS e NTS e manejo agrícola na área de estudo.

Palavras-chave: Irrigação por microaspersão. Resíduo de poda. San Joaquin Valley. Saúde do solo. Tulare county.

2.1 INTRODUCTION

California is the leading state on agriculture production in the United States of America. The state produces food on about 9.9 million ha of agricultural land, whereupon 4.7 million ha are pastureland, and about 3.8 million ha are cropland (USDA-NASS, 2017). With 69,400 farms and ranches, California agriculture generated a total cash receipt of $49.9 billion over the production of a wide variety of commodities (CDFA, 2019). The top three agricultural counties in California are Fresno ($7.9 billion), Kern ($7.5 billion), and Tulare ($7.2 billion), with a total value of about $22.6 billion (CDFA, 2019).

The citrus production in California accounted for 54% of the total country production, followed by Florida with 42%, and Texas and Arizona with 4% (USDA-NASS, 2020). The counties of Fresno, Kern, and Tulare are leaders in the production of oranges (navel) and mandarins, being Tulare the leader for both ranks with a total acreage of about 26,673 hectares for oranges and 9,696 hectares for mandarins (CDFA, 2020a). These three counties are in the San Joaquin Valley, which is the major agricultural production region in the state of California.

As an evergreen perennial crop, citrus requires additional water throughout the year to attend to the water needs in the Mediterranean climate of the region and to comply with the national and world food demands. However, San Joaquin Valley has been facing periodic droughts and environmental policies, resulting in significant declines in water supplies for the irrigated crops (MARINO et al., 2019). Soil organic carbon (SOC) and soil total nitrogen (STN) also play and an important role in agriculture productivity,

by providing nutrients for crop development and promoting the physical structure of soils (WANG et al., 2016).

SOC is an important element of the solid fraction of soils, and it involves a mixture of plant and animal residues and microbial biomass under different stages of decomposition (LAL, 2018), and by-products from microbial processes (ANTHONY et al., 2020). The interest in SOC dynamics is increasing because it is the major indicator of soil fertility, and develops a crucial role in carbon dioxide sequestration (SCHILLACI et al., 2019). As an indicator of soil health, SOC is receiving significant attention from the farming community, state agencies, initiatives, and organizations, such as the Food and Agriculture Organization of the United Nations (FAO, 2020), the “4 per 1000” initiative (FRENCH MINISTRY OF AGRICULTURE & FOOD, 2020), and California’s Healthy Soils Initiative (CDFA, 2020c).

Total nitrogen includes different forms of nitrogen, such as nitrate, nitrite, ammonia, ammonium, and organic nitrogen (EPA, 2013). The uptake assimilation of soil nitrogen by plants occurs in the forms of nitrate (NO_3^-) and ammonium (NH_4^+), which are essential components that can be used to produce nucleic acids, proteins, and chlorophylls (RUAN et al., 2016). As SOC, soil total nitrogen (STN) is an indicator of soil fertility, being associated with crop productivity and food security (ZHOU et al., 2019). Therefore, reliable measurements and spatial analysis of SOC and STN are crucial for efficient agricultural management.

There are many examples of studies about SOC and STN distribution conducted among different ecosystems, such as forests (MA et al., 2020; WANG et al., 2016), grassland and farmland (XUE; AN, 2018), shrub land (XUE; AN, 2018; WANG et al., 2016), field crops (LIU et al., 2021; WANG et al., 2016), and apple orchards (ZHANG et al. 2021). Previous studies focused on SOC content and stock of citrus orchards considering different tree ages, soil sampling depths, and orchard management (CANALI et al., 2009; OLIVEIRA et al., 2015; GU et al., 2016; NOVARA et al., 2019). However, there are no examples of research regarding the distribution of SOC and STN across tree transects in citrus orchards.

The general objective of this study was to characterize the multi-scale (tree and orchard) variability of SOC and STN over mature micro-irrigated citrus orchards, grown under the same soil conservation practice, in California’s San Joaquin Valley (USA). Additionally, the study aimed to verify if the citrus orchards result in similar spatial

patterns of SOC, STN, plant total carbon (PTC), and plant total nitrogen (PTN), across the soil groups.

2.2 MATERIAL AND METHODS

2.2.1 Description of the study area

Two commercial citrus orchards were selected for this research, both located in Tulare County (in the southeastern portion of San Joaquin Valley), California. The first study site is a Page mandarin (*Citrus reticulata*) orchard in Strathmore, CA, while the second is a Washington navel orange (*Citrus sinensis*) orchard in Ivanhoe, CA (Figure 1).

Figure 1 - Overview of the study area, indicating the a) geographic location in Tulare county, state of California (USA); b) sampling locations at the orchard in Ivanhoe; c) sampling locations at the orchard in Strathmore (orange points represent the sampling locations in soil group 1, green in soil group 2, and blue in soil group 3)

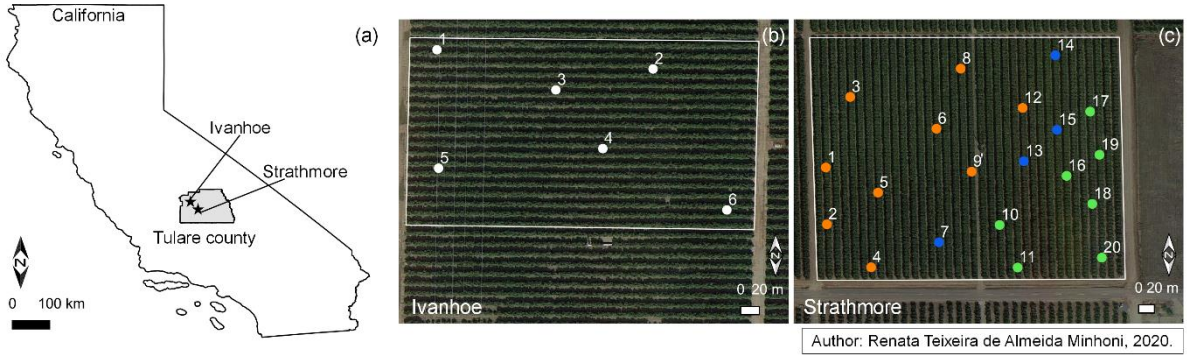

Both orchards are under a Mediterranean climate (California's climate zone number 13) and are under the same soil conservation practice. Both orchards are irrigated with micro-sprinklers (fanjets), with irrigation scheduling that is based on a combination of soil moisture monitoring and evapotranspiration (ET), using grass reference evapotranspiration (ET_o) taken from the network of automated weather stations of the California Irrigation Management Information System (CIMIS), and crop coefficient (Kc) value around 0.7 throughout the irrigation season. The residues from pruning processes are mechanically shredded and left onto the ground of the inter-rows.

The study site in Strathmore is located between the latitudes 36°10'02.45"N and 36°10'09.53"N and the longitudes 119°01'22.70"W and 119°01'31.70"W, at an average

elevation of 142 meters. The orchard is four ha in size (200 m x 200 m) and consists of 11-year old trees planted at 2.5 m x 5.5 m spacing, with North-South row orientation, and with Paige variety grafted onto Carrizo citrange rootstock. The mandarin trees are planted on berms or ridges (raised mounds of soil), with around 0.4 m in height. The study site in Ivanhoe is located between the latitudes 36°23'09.67"N and 36°23'14.10"N and the longitudes 119°14'26.10"W and 119°14'33.86"W, at an average elevation of 107 meters. The orchard is 2.2 ha in size (120 m x 185 m) and consists of 20-year old trees planted at 3.0 m x 6.5 m spacing with East-West row orientation, and with Washington navel variety grafted onto Trifoliate rootstock.

2.2.2 Soil parameters dataset

The soil sampling scheme was selected using the Response Surface Sampling Design (RSSD) methodology with the ECe Sampling Assessment and Prediction (ESAP) software (LESCH et al., 2000), which is a free software (ESAP-RSSD) developed by the United States Department of Agriculture – Agriculture Research Service (USDA-ARS). The ESAP-RSSD determines the optimized soil sampling locations that best characterize the frequency statistics of the geospatial sensor data (SCUDIERO et al., 2019).

For the orchard in Strathmore, multispectral imagery data, collected with an unmanned aerial vehicle (UAV), was used to identify 20 representative locations (see Scudiero et al., 2019 for additional information) (Figure 1c). For the orchard in Ivanhoe, six soil sampling locations were selected using geospatial soil apparent electrical conductivity (ECa) measurements obtained with a handheld EM38 (Geonics Ltd.) in the vertical mode (e.g., sensing the 0-1.5m soil profile) connected to a GPS, according to recommendations provided by Corwin and Scudiero (2016) (Figure 1b).

The field research team collected the soil samples on 10-12 December 2019, based on a transects survey to determine soil parameters (SOC and STN) and contrast the small scale (tree) characteristics with the larger scale (orchard) features. Each transect was divided into three sections: 1) section α was located at 0.6 m from the tree trunk; 2) section β was at 1.2 m from the trunk (below the projection of the tree canopy); and 3) section γ was in the center of the inter-row (Figure 2). At each section, the soil was sampled at two soil layers, from 0-0.05 m and 0.05-0.4 m, totaling six soil samples at each transect. Therefore, soil samples were collected from 20 transects (towards East)

at the orchard in Strathmore, and from six transects (towards North) at the orchard in Ivanhoe, totaling 156 soil samples (120 collected in Strathmore and 36 in Ivanhoe). Each sample had approximately 0.5 kg of soil. SOC and STN were analyzed by the UC Davis Analytical Laboratory (https://anlab.ucdavis.edu/), through a combustion method using a LECO TruMac CN Analyzer. Samples were also analyzed for gravimetric soil water content (SWC).

Figure 2 - Representation showing the transect and the soil sampling sections (α, β, and γ)

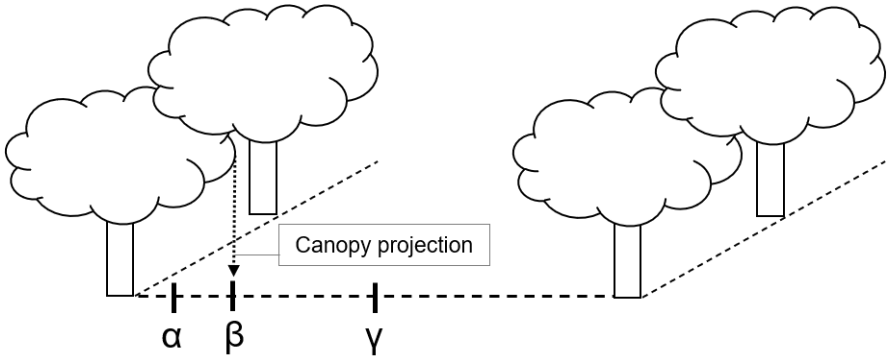

2.2.3 Plant tissue dataset

In December 2019, concurrently with the soil survey, plant tissue samples were collected at the 20 trees in Strathmore and six trees in Ivanhoe. The sampling methodology was based on the document from Obreza et al. (2018) and the protocol recommended by the California Department of Food and Agriculture (CDFA, 2020b). Briefly, the leaves were sampled from each quadrant of the tree, from about 0.9 to 1.5 m above the ground, and from the spring flush (medium-sized, and narrow and pointed appearance). The samples were analyzed for plant total carbon (PTC) and plant total nitrogen (PTN), using a LECO TruMac CN Analyzer from the UC Davis Analytical Laboratory.

2.2.4 Data analysis

The statistical analyses were performed using Excel (Microsoft Office 2016) and RStudio Version 1.3.959 (R CORE TEAM, 2020). The differences in soil parameters among the multi-scale were tested using the Kruskal-Wallis (KW) test (KRUSKAL;

WALLIS, 1952). The KW is a non-parametric test, that can be used instead of the classical analysis of variance (ANOVA) when the assumptions for a parametric test were not met. The differences across plant tissue parameters were also carried out using the KW test. Comparisons between means were performed by Kruskal-Wallis multiple comparison tests, with statistical significance at p-value < 0.05, using the package pgirmess version 1.6.9 (GIRAUDOUX, 2018) in the RStudio (R CORE TEAM, 2020). Linear regressions were conducted to verify the relationship between SOC, STN, and SWC.

2.3 RESULTS AND DISCUSSION

2.3.1 Analysis for multi-scale SOC and STN

The multi-scale SOC and STN were analyzed by contrasting the representativeness of a larger scale, characterized by the orchard, with a smaller scale, characterized by the tree transects (Figures 3 and 4). The orchard in Strathmore showed significantly greater mean values of SOC and STN from 0.05 to 0.40 m and from 0 to 0.40 m compared with the orchard in Ivanhoe. At the whole soil profile, the SOC mean value at Strathmore was 79.9% greater than in Ivanhoe, and the STN mean value at Strathmore was 31.4% greater than in Ivanhoe. From 0 to 0.05 m, SOC and STN mean values did not show a significant difference between the orchards.

Figure 3 - Boxplots of soil organic carbon (SOC, %) distribution along with the orchard and the tree scale (sampling sections α, β, and γ). Boxplots (a), (c), and (e) indicate the SOC distribution from 0 to 0.05 m, from 0.05 to 0.40 m, and from 0 to 0.40 m, respectively, at the orchard in Strathmore. Boxplots (b), (d), and (f) indicate the SOC distribution at the same depths at the orchard in Ivanhoe. The boxes topped with lowercase letters indicate the multiple comparisons, from Kruskal–Wallis multiple comparison tests, within the tree sampling sections, and the upper-case letters between the orchard and the sections. Different lowercase or upper-case letters indicate that the mean values are significantly different (p-value < 0.05). Boxes with no topped letters indicate a non-significant difference

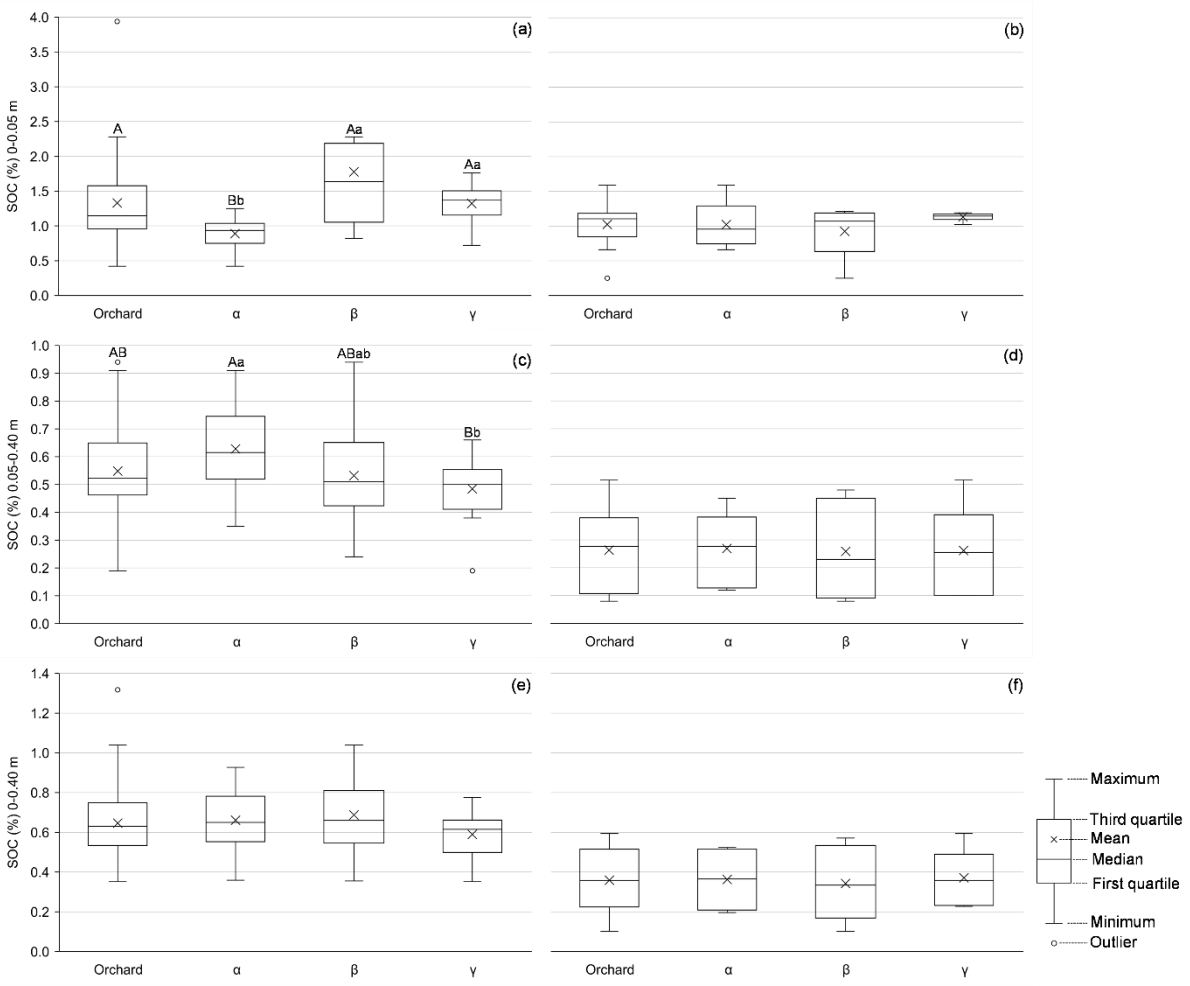

Figure 4 - Boxplots of soil total nitrogen (STN, %) distribution along with the orchard and the tree scale (sampling sections α, β, and γ). Boxplots (a), (c), and (e) indicate the STN distribution from 0 to 0.05 m, from 0.05 to 0.40 m, and from 0 to 0.40 m, respectively, at the orchard in Strathmore. Boxplots (b), (d), and (f) indicate the SOC distribution at the same depths at the orchard in Ivanhoe. The boxes topped with lowercase letters indicate the multiple comparisons, from Kruskal–Wallis multiple comparison tests, within the sections and the upper-case letters between the orchard and the sections. Different lowercase or upper-case letters indicate that the mean values are significantly different (p-value < 0.05). Boxes with no topped letters indicate a non-significant difference

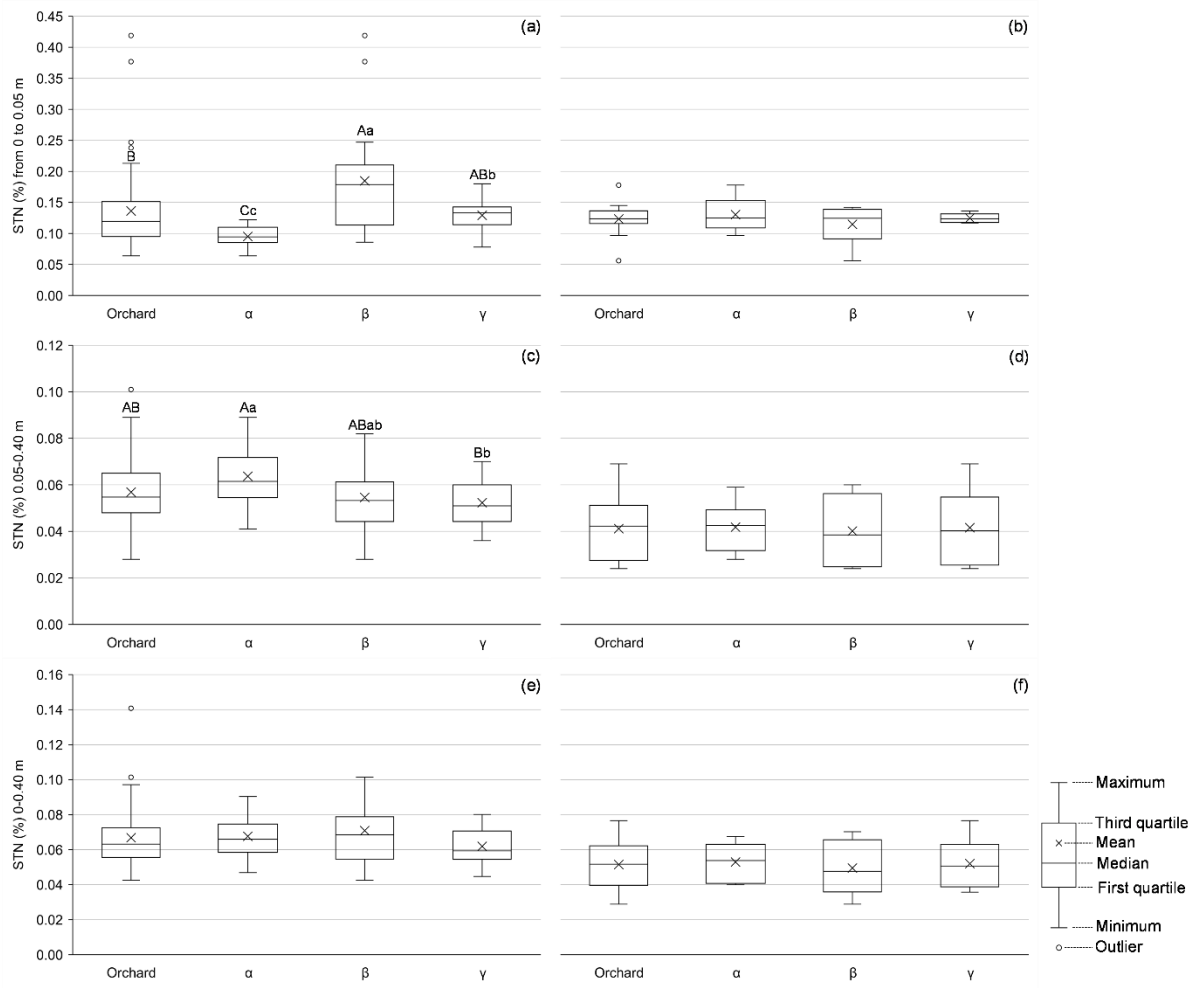

The orchard in Strathmore is predominantly characterized by loam and clay loam soil. Whereas in Ivanhoe, the orchard presents a sandier soil. Jagadamma and Lal (2010) found that the clay fraction of the soil accumulates more SOC, followed by the silt, and the sand fractions. Soil with higher concentrations of clay is prone to have a higher specific surface area for organic matter adsorption (POIRIER et al., 2020), being the clay particle the most active element in the development of organo-mineral

complexes (CHENU et al., 2016). The silt and clay-sized particles can protect soil organic matter from decomposition, due to the formation of aggregates between these elements (HASSINK, 1997). The observations of Zhang et al. (2016) from a study conducted along the Dan river valley in China, indicated that STN, ammonium (NH_4^+), and nitrate (NO_3^-) showed a negative correlation with sand, but a positive correlation with clay and silt. The mentioned findings are consistent with the results obtained in this research, where higher concentrations of SOC and STN were found in the orchard with a greater amount of clay.

At the orchard in Strathmore, significant statistical differences were found for SOC from 0 to 0.05 m and from 0.05 to 0.40 m. From 0 to 0.05 m, the sampling sections α, β, and γ showed SOC mean values of 0.887%, 1.777%, and 1.322%, respectively. Sections β and γ were representatives of the orchard, which presented a mean value of 1.329%. From 0.05 to 0.40 m, the sections α, β and γ showed SOC mean values of 0.629%, 0.532%, and 0.485%, respectively. At this soil layer, all the sampling sections were representative of the orchard, which presented a mean value of 0.548%. Considering the entire soil profile layer, from 0 to 0.40 m, no significant difference was detected for SOC within the tree sampling sections, and between the orchard and the sections. At this layer, the mean SOC values for the orchard and sections α, β, and γ, were 0.646%, 0.661%, 0.688%, and 0.589%, respectively. It indicates that the application of the pruning residues in the inter-rows showed a positive effect on the SOC content.

At the same orchard, significant statistical differences were also found for STN from 0 to 0.05 m and from 0.05 to 0.40 m. From 0 to 0.05 m, the sampling sections α, β, and γ showed STN mean values of 0.095 %,0.185%, and 0.129%, respectively. Only section γ was representative of the orchard, which presented a mean value of 0.136%. From 0.05 to 0.40 m, the sections α, β and γ showed STN mean values of 0.064%, 0.055%, and 0.052%, respectively. At this soil layer, all the sampling sections were representative of the orchard, which presented a mean value of 0.057%. At the entire studied soil profile, from 0 to 0.40 m, no significant difference was detected within the tree transect sections, and among the orchard and the sections. At this soil profile, the mean STN values for the orchard and sections α, β, and γ, were 0.067%, 0.068%, 0.071%, and 0.062%, respectively.

From 0 to 0.05 m, section β showed a higher mean value for SOC and STN content, whereas section α showed a lower mean value for both soil parameters. The

berms may have a significant influence on these results. The berms in heavier soils (clay and silt soils) can minimize the soil water holding capacity and the occurrence of the Phytophthora root rot, which can be caused under conditions of high soil moisture and deficient drainage (FABER; GOLDHAMER, 2014). Phytophthora species can cause Citrus gummosis in situations of moistened trunks, and it can be reduced by avoiding soil retention and guaranteeing aeration around the tree trunk (FABER; GOLDHAMER, 2014). In section α, SOC and STN maybe eventually lost from stormwater or irrigation runoff over the berms, towards the base of the berm at section β. Additionally, it was found pruning residues not only at section γ but also at section β.

From 0.05 to 0.40 m and 0 to 0.40 m, the higher mean values for SOC and STN concentrations were found in sections α and β. The micro-sprinkler irrigation system delivers nutrients to the citrus trees through fertigation, where the required nutrients are applied under the canopy area. The maximum concentration of the citrus roots is located under the tree canopy. Generally, plant roots material interferes in the SOC pool, by adding organic carbon through dead roots and rhizodeposition (DIJKSTRA et al., 2020). Citrus trees have a matted layer of fibrous roots just below the soil surface, whose function is to absorb water and nutrients (FREELAND, 2016). These facts reflect the higher mean values of SOC and STN at the transect sampling sections below the citrus canopy.

At the orchard in Ivanhoe, no statistical difference was detected between the orchard and the transects sections, and within the sections. Therefore, for the three examined soil depths, all the sampling sections (α, β, and γ) for SOC and STN were representative of the entire orchard. The frequency distribution of these parameters indicates that the orchard in Ivanhoe is more homogenous than the orchard in Strathmore. This result agrees with the smaller amount of sampling locations indicated by the ESAP-RSSD software. Considering the whole soil profile (0 to 0.40 m), the SOC mean values were similar across the boxplots (0.359% for the orchard, 0.363% for section α, 0.342% for section β, and 0.371% for section γ). The STN mean values were also similar across the boxplots from 0 to 0.40 m (0.051% for the orchard, 0.053% for section α, 0.049% for section β, and 0.052% for section γ).

2.3.2 Analysis for soil groups

An analysis across the three distinct soil groups and each section of the transect were conducted to investigate the possible SOC and STN differences at the Strathmore's citrus orchard (Figure 5). Significant statistical differences were found only in the first five centimeters of the soil. At this soil layer, the higher mean values of SOC and STN were found in section β, followed by section γ, and section α. No significant statistical differences were found in SOC and STN across the soil groups of each section. Additionally, the mean values of PTC and PTN were similar along with the soil groups, with no significant statistical differences.

Figure 5 - Boxplots of soil organic carbon (SOC, %) from 0 to 0.05 m (a), from 0.05 to 0.40 m (b), and from 0 to 0.40 m (c), soil total nitrogen (STN, %) from 0 to 0.05 m (d), from 0.05 to 0.40 m (e), and from 0 to 0.40 m (f) along the sections (α, β, and γ) and according to the soil groups (SG1 = soil group 1, SG2 = soil group 2, and SG3 = soil group 3) at Strathmore. The boxes topped with letters indicate the Kruskal-Wallis multiple comparison within each soil group. Different letters indicate that the mean values are significantly different (p-value < 0.05). Boxes with no topped letters indicate a non-significant difference

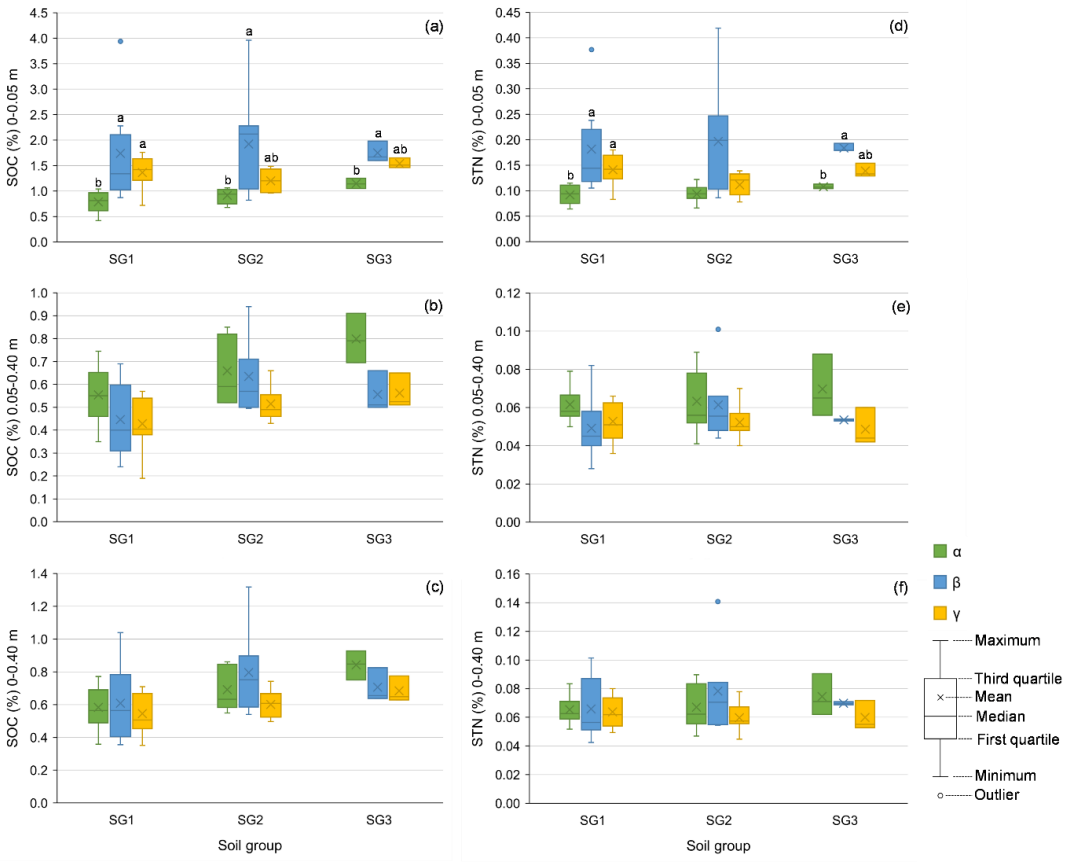

2.3.3 Relationship analysis between soil parameters

Based on relationship analysis, the positive linear regressions between SOC and STN, SOC and SWC, and STN and SWC are illustrated in Figure 6. The regression between SOC and STN revealed a very strong relationship along the three soil layer depths at the orchard in Ivanhoe. At Strathmore's orchard, a very strong relationship was found from 0 to 0.05 m, a strong from 0 to 0.40 m, and a moderate from 0.05 to 0.40 m.

The results indicate that the relationships between SOC and STN at the orchard in Ivanhoe (Figure 6b) are better coupled than the orchard in Strathmore (Figure 6a), which was expected as Ivanhoe has a more homogeneous soil. In general, there is a high correlation between SOC and TN in the soil, which enables us to make assumptions about SOC based on STN and vice versa (WINOWIECKI et al., 2015). The findings from this study are consistent with the results from other studies over different environments. Cheng et al. (2016) obtained a positive and very strong linear correlation (R^2 = 0.99) in a rice paddy area in Japan, where the authors collected soil samples from 0 to 0.25 m. Xue et al. (2018) investigated the relationship between SOC and STN from 0 to 0.6 m of soil depth along different land uses in a watershed in China. The authors reported positive correlations in farmland (r = 0.61), abandoned farmland (r = 0.79), Shrub land (r = 0.82), and natural grassland (r = 0.93). Across different agroecosystems in China, Zhai et al. (2019) observed significant positive correlations from 0 to 0.1 m (R^2 = 0.99), from 0.1 to 0.2 m (R^2 = 0.75), and from 0.2 to 0.3 m (R^2 = 0.88).

At Strathmore's orchard, a very weak significant relationship was detected between SOC and SWC. A very weak significant relationship was found between STN and SWC from 0 to 0.05, and a non-significant relationship from 0.05 to 0.40 and from 0 to 0.40 m. At Ivanhoe's orchard, a weak significant relationship was observed between SOC and SWC. A moderate significant relationship was identified among STN and SWC from 0 to 0.05 m and a weak significant from 0.05 to 0.40 m and from 0 to 0.40 m.

Figure 6 - Linear regression between soil organic carbon (SOC, %) and soil total nitrogen (STN, %), SOC and soil water content (SWC, m^3 m^{-3}), and STN and SWC, from 0 to 0.05 m, 0.05 to 0.40 m, and 0 to 0.40 m, at Strathmore (a, c, and e) and Ivanhoe (b, d, and f). R^2 represents the coefficient of determination. *, ** and * denotes significant relationship at p-value < 0.001, p-value < 0.01 and p-value < 0.05, respectively**

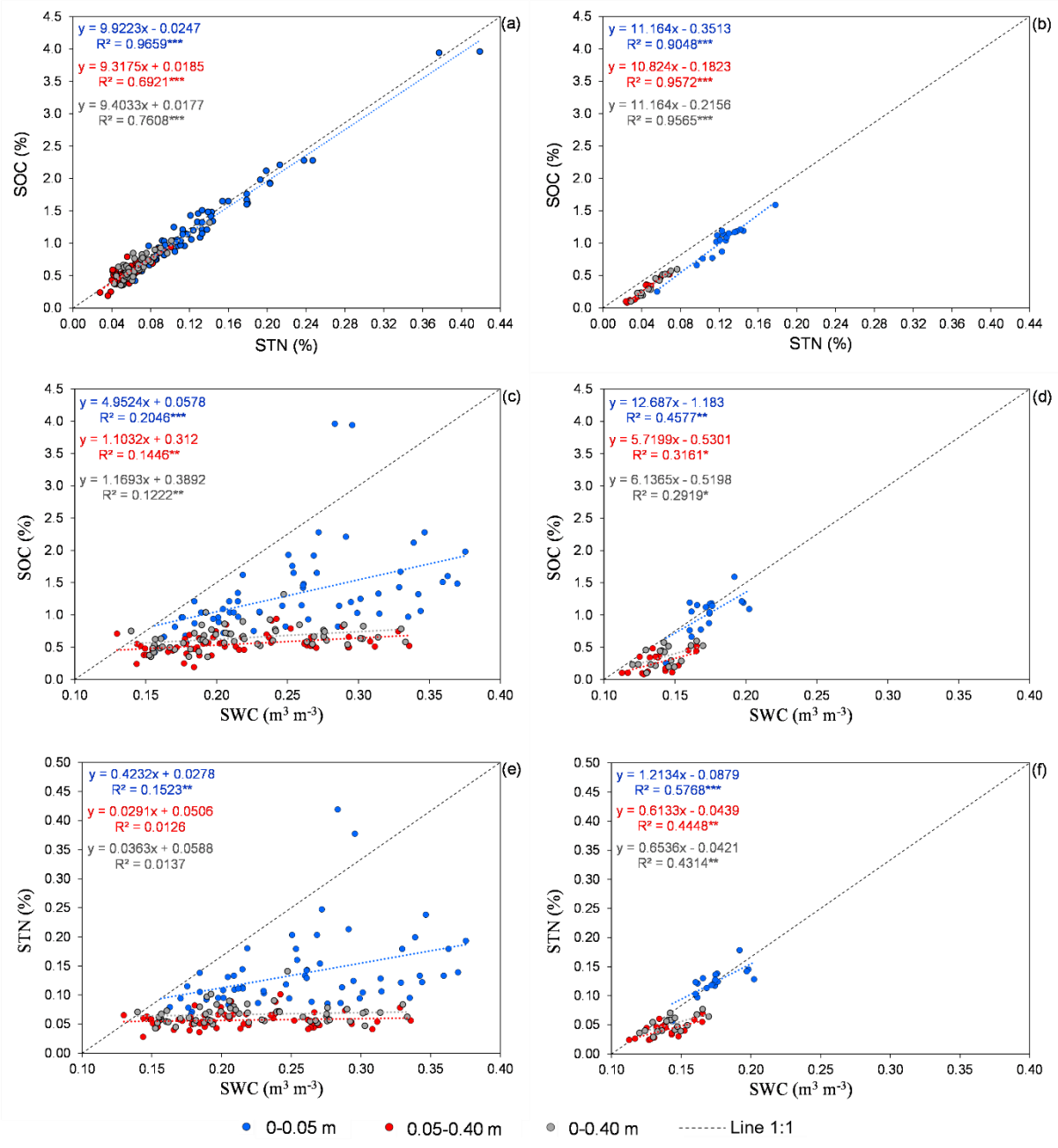

2.4 CONCLUSIONS

Regardless of the same soil conservation practice, the study areas revealed different patterns on SOC and STN. Such differences may be due to the soil groups in

the areas. Ivanhoe, which represents a more homogeneous area characterized by one soil group, did not show significant differences on SOC and STN levels. Whereas Strathmore, with three different soil groups, showed statistical differences.

Characterizing the multi-scale variability of SOC and STN in mature macro-irrigated citrus orchards is relevant for the future project development of SOC and STN monitoring and best agricultural management practices. Future research should focus on the investigation of the spatial variability of SOC and STN stock, on multi-year comparisons, and on the impact of different conservation practices, such as the use of cover crops in the inter-rows.

REFERENCES

ANTHONY, M. A.; CROWTHER, T. W.; MAYNARD, D. S.; VAN DEN HOOGEN, J.; AVERILL, C. Distinct Assembly Processes and Microbial Communities Constrain Soil Organic Carbon Formation. **One Earth** 2, 4, 349–360, 2020.

CANALI, S.; DI BARTOLOMEO, E.; TRINCHERA, A.; NISINI, L.; TITTARELLI, F.; INTRIGLIOLO, F.; ROCCUZZO, G.; CALABRETTA, M. L. Effect of different management strategies on soil quality of citrus orchards in Southern Italy. **Soil Use and Management** 25, 1, 34–42, 2009.

CDFA. California Department of Food and Agriculture. **Agricultural Statistics Review 2018-2019**, 2019. Available in: https://www.cdfa.ca.gov/statistics/PDFs/2018-2019AgReportnass.pdf. Accessed on: 16 December 2020.

CDFA. California Department of Food and Agriculture. **California Citrus Acreage Report**, 2020a. Available in: https://www.nass.usda.gov/Statistics_by_State/California/Publications/Specialty_and_Other_Releases/Citrus/Acreage/202008citac.pdf. Accessed on: 16 December 2020.

CDFA. California Department of Food and Agriculture. **California Fertilization Guidelines: Citrus**, 2020b. Available in: https://www.cdfa.ca.gov/is/ffldrs/frep/FertilizationGuidelines/Citrus.html#N. Accessed on: 01 December 2020.

CDFA. California Department of Food and Agriculture. **California's healthy soils initiative**, 2020c. Available in: https://www.cdfa.ca.gov/healthysoils/. Accessed on: 20 December 2020.

CHENG, W.; PADRE, A. T.; SATO, C.; SHIONO, H.; HATTORI, S.; KAJIHARA, A.; AOYAMA, M.; TAWARAYA, K.; KUMAGAI, K. Changes in the soil C and N contents, C decomposition and N mineralization potentials in a rice paddy after long-term application of inorganic fertilizers and organic matter. **Soil Science and Plant Nutrition**, 62, 2, 212–219, 2016.

CHENU, C.; PLANTE, A. F.; PUGET, P. Organo-mineral relationships. *In*: LAL, R., **Encyclopedia of Soil Science**, 3rd ed., CRC Press: Boca Raton, FL, USA, 2016. p. 1227–1230.

CORWIN, D. L.; SCUDIERO, E. Field-Scale Apparent Soil Electrical Conductivity. *In*: LOGSDON, S. (Ed.), **Methods of Soil Analysis**. Soil Science Society of America, Madison, WI, USA, 2016. p. 1-29.

DIJKSTRA, F. A.; ZHU, B.; CHENG, W. Root effects on soil organic carbon: a double-edged sword. **New Phytologist**, 2020.

EPA. Environmental Protection Agency. **Total nitrogen**, 2013. Available in: https://www.epa.gov/sites/production/files/2015-09/documents/totalnitrogen.pdf. Accessed on: 20 December 2017.

FABER, B.; GOLDHAMER, D. A. Irrigation. *In*: FERGUSON, L.; GRAFTON-CARDWELL, E. E. (Eds.), **Citrus production manual**. University of California. Division of Agriculture and Natural Resources. Communication Services, Richmond, CA, 2014. p. 183-196.

FAO. Food and Agriculture Organization of the United Nations. **Global soil partnership: Soil organic carbon**, 2020. Available in: http://www.fao.org/global-soil-partnership/areas-of-work/soil-organic-carbon/en/. Accessed on: 20 December 2020.

FREELAND, R. S. Surveying the near-surface fibrous citrus root system of the orange tree with 3-D GPR. **Applied Engineering in Agriculture** 32, 2, 145-153, 2016.

FRENCH MINISTRY OF AGRICULTURE AND FOOD. **4 pour 1000 initiative**, 2020. Republique Francaise, Montpellier, France. Available in: https://www.4p1000.org/. Accessed on: 20 December 2020.

GIRAUDOUX, P.; ANTONIETTI, J.; BEALE, C.; PLEYDELL., D.; TREGLIA, M. **Package 'pgirmess'**. Version 1.6.9, 2018. Available in: https://cran.r-project.org/web/packages/pgirmess/index.html. Accessed on: 15 November 2020.

GU, C.; LIU, Y.; MOHAMED, I.; ZHANG, R.; WANG, X.; NIE, X.; JIANG, M.; BROOKS, M.; CHEN, F.; LI, Z. Dynamic Changes of Soil Surface Organic Carbon under Different Mulching Practices in Citrus Orchards on Sloping Land. **Plos One** 11, 12, e0168384, 2016.

HASSINK, J. The capacity of soils to preserve organic C and N by their association with clay and silt particles. **Plant and Soil** 191, 77–87, 1997.

JAGADAMMA, S.; LAL, R. Distribution of organic carbon in physical fractions of soils as affected by agricultural management. **Biology and Fertility of Soils** 46, 543–554, 2010.

KRUSKAL, W. H.; WALLIS, W. A. Use of ranks in one-criterion variance analysis. **Journal of the American Statistical Association** 47, 583–621, 1952.

LAL, R. Digging deeper: A holistic perspective of factors affecting soil organic carbon sequestration in agroecosystems. **Global Change Biology** 24, 3285–3301, 2018.

LESCH, S. M. Sensor-directed response surface sampling designs for characterizing spatial variation in soil properties. **Computers and Electronics in Agriculture**, 46, 153–179, 2005.

LIU, N.; LI, Y.; CONG, P.; WANG, J.; GUO, W.; PANG, H.; ZHANG, L. Depth of straw incorporation significantly alters crop yield, soil organic carbon and total nitrogen in the North China Plain. **Soil and Tillage Research** 205, 104772, 2021.

MA, T.; LIU, X.; XU, S.; GUO, H.; HUANG, H.; HU, C.; WU, D.; SUN, Z.; CHEN, C.; SONG, W. Levels and variations of soil organic carbon and total nitrogen among

forests in a hotspot region of high nitrogen deposition. **Science of the Total Environment** 713, 136620, 2020.

MARINO, G.; ZACCARIA, D.; SNYDER, R. L.; LAGOS, O.; LAMPINEN, B. D.; FERGUSON, L.; GRATTAN, S. R.; LITTLE, C.; SHAPIRO, K.; MASKEY, M. L.; CORWIN, D. L.; SCUDIERO, E.; SANDEN, B. L. Actual Evapotranspiration and Tree Performance of Mature Micro-Irrigated Pistachio Orchards Grown on Saline-Sodic Soils in the San Joaquin Valley of California. **Agriculture** 9, 4, 76, 2019.

NOVARA, A.; PULIDO, M.; RODRIGO-COMINO, J.; DI PRIMA, S.; SMITH, P.; GRISTINA, L.; GIMÉNEZ-MORERA, A.; TEROL, E.; SALESA, D.; KEESSTRA, S. Long-term organic farming on a citrus plantation results in soil organic carbon recovery. **Cuadernos de Investigación Geográfica** 45, 1, 271-286, 2019.

OBREZA, T. A.; ZEKRI, M.; HANLON, E. A.; MORGAN, K.; SCHUMANN, A.; ROUSE, R. **Soil and Leaf Tissue Testing for Commercial Citrus Production**. SL253.04, Cooperative Extension Service, University of Florida, Institute of Food and Agricultural Sciences: Gainesville, FL, USA, 2018.

OLIVEIRA, F. É. R.; OLIVEIRA, J. M.; XAVIER, F. A. S. Changes in Soil Organic Carbon Fractions in Response to Cover Crops in an Orange Orchard. **Revista Brasileira de Ciência do Solo** 40, e0150105, 2016.

POIRIER, V.; BASILE-DOELSCH, I.; BALESDENT, J.; BORSCHNECK, D.; WHALEN, J.K.; ANGERS, D. A. Organo-Mineral Interactions Are More Important for Organic Matter Retention in Subsoil Than Topsoil. **Soil Systems** 4, 4, 2020.

R CORE TEAM. **R: A language and environment for statistical computing**. R Foundation for Statistical Computing, Vienna, Austria, 2020.

RUAN, L.; WEI, K.; WANG, L.; CHENG, H.; ZHANG, F.; WU, L.; BAI, P.; ZHANG, C. Characteristics of NH_4^+ and NO_3^- fluxes in tea (Camellia sinensis) roots measured by scanning ion-selective electrode technique. **Scientific Reports** 6, 38370, 2016.

SCHILLACI, C.; ACUTIS, M.; VESELY, F.; SAIA, S. A simple pipeline for the assessment of legacy soil datasets: An example and test with soil organic carbon from a highly variable area. **Catena** 175, 110-122, 2019.

SCUDIERO, E.; ZUNIGA, G.; POURREZA, A. Using the ESAP-RSSD Software to Direct Citrus Tree Sampling with Aerial Multispectral Data. **FastTIMES** 24, 4, 130-133, 2019.

USDA-NASS. United States Department of Agriculture, National Agricultural Statistics Service. **2017 Census of Agriculture: State Profile, California**, 2017. Available in: https://www.nass.usda.gov/Publications/AgCensus/2017/Online_Resources/County_Profiles/California/cp99006.pdf. Accessed on: 16 December 2020.

USDA-NASS. United States Department of Agriculture, National Agricultural Statistics Service. **Citrus Fruits: 2020 Summary**. United States Department of Agriculture, Washington D.C., 2020. Available in: https://ccqc.org/wp-content/uploads/USDA-Citrus-Fruits-Summary-82620.pdf. Accessed on: 16 December 2020.

WANG, J.; BAI, J.; ZHAO, Q.; LU, Q.; XIA, Z. Five-year changes in soil organic carbon and total nitrogen in coastal wetlands affected by flow-sediment regulation in a Chinese delta. **Scientific Reports** 6, 1, 2016.

WANG, T.; KANG, F.; CHENG, X.; HAN, H.; JI, W. Soil organic carbon and total nitrogen stocks under different land uses in a hilly ecological restoration area of North China. **Soil & Tillage Research** 163, 176–184, 2016.

WINOWIECKI, L., VÅGEN, T., MASSAWE, B., JELINSKI, N. A., LYAMCHAI, C., SAYULA, G., MSOKA, E. Landscape-scale variability of soil health indicators: effects of cultivation on soil organic carbon in the Usambara Mountains of Tanzania. **Nutrient Cycling in Agroecosystems** 105, 3, 2015.

XUE, Z.; AN, S. Changes in soil organic carbon and total nitrogen at a small watershed scale as the result of land use conversion on the Loess Plateau. **Sustainability** 10, 4757, 2018.

ZHANG, J.; LI, P.; JIA, C.; LI, Z.; TANG, H.; YANG, Y. Distribution of soil nitrogen and its relationship with particle size along the Dan river valley, China. **Environmental Earth Sciences** 75, 406, 2016.

ZHANG, Y.; WANG, R.; PENG, X.; ZHANG, Y.; NING, F.; XU, Z.; WANG, Q.; DONG, Z.; JIA, G.; WEI, L.; LI, J. Changes in soil organic carbon and total nitrogen in apple orchards in different climate regions on the Loess Plateau. **Catena** 197, 104989, 2021.

ZHAI, X.; LIU, K.; FINCH, D. M.; HUANG, D.; TANG, S.; LI, S.; LIU, H.; WANG, K. Stoichiometric characteristics of different agroecosystems under the same climatic conditions in the agropastoral ecotone of northern China. **Soil Research** 57, 8, 875, 2019.

ZHOU, T.; GENG, Y.; CHEN, J.; SUN, C.; HAASE, D.; LAUSCH, A. Mapping of Soil Total Nitrogen Content in the Middle Reaches of the Heihe River Basin in China Using Multi-Source Remote Sensing-Derived Variables. **Remote Sensing** 11, 2934, 2019.

GENERAL CONSIDERATIONS

Towards the scenario of an increasing global population and climate change, maintaining and enhancing soil health are important goals to the achievement of sustainable agriculture, crop productivity, climate resilience, and food security. Conservation agricultural practices, such as no-till or reduced tillage, crop rotation, and retention of crop residues, tend to improve soil health by the increase in SOC levels, nutrient cycling, and soil biota.

The conventional methods for SOC monitoring and evaluation are labor-intensive, time-consuming, and costly. This laborious task can be overcome by the application of remote sensing techniques, which can provide rapid and low-cost methods for SOC measurement. The adoption of multitemporal spectral indices analysis over Sentinel-2 images provides a higher accuracy assessment of topsoil SOC proxies at the Brazilian study area, relative to the use of single-date images.

As SOC, STN is also a key element for soil fertility, and for plant growth and development. Therefore, the spatial variability of both soil parameters is needed for monitoring and management issues. For an appropriate measurement, the soil samples should be representative of the entire studied area, which may vary with different factors, such as soil sampling depth and location, soil type, and agricultural management.

In San Joaquin Valley (California), citrus orchards resulted in different spatial variability of SOC and STN. Although the orchards were under the same management, they were over different soil groups. Therefore, the representativeness of the sampling locations was different among the orchards, which straights the needs of sampling studies before the elaboration of projects, and agricultural and environmental management strategies development.

REFERENCES

ANA. Agência Nacional de Águas. **Atlas irrigação: Uso da água na agricultura irrigada**. Brasília: ANA, 2017.

ANGELAKIS, A. N.; ZACCARIA, D.; KRASILNIKOFF, J.; SALGOT, M.; BAZZA, M.; ROCCARO, P.; JIMENEZ, B.; KUMAR, A.; YINGHUA, W.; BABA, A.; HARRISON, J. A.; GARDUNO-JIMENEZ, A.; FERERES, E. Irrigation of World Agricultural Lands: Evolution through the Millennia. **Water** 12, 5, 1285, 2020.

ANGELOPOULOU, T.; TZIOLAS, N.; BALAFOUTIS, A.; ZALIDIS, G.; Bochtis, D. Remote sensing techniques for soil organic carbon estimation: A review. **Remote Sensing** 11, 676, 2019.

CDFA. California Department of Food and Agriculture. California Agricultural Production Statistics, **2019 Crop Year – Top 10 Commodities for California Agriculture**, 2020. Available in: https://www.cdfa.ca.gov/Statistics/. Accessed on: 28 December 2020.

CHENU, C.; ANGERS, D. A.; BARRÉ, P.; DERRIEN, D.; ARROUAYS, D.; BALESDENT, J. Increasing organic stocks in agricultural soils: Knowledge gaps and potential innovations. **Soil and Tillage Research** 188, 2019.

DELUZ, C.; NUSSBAUM, M.; SAUZET, O.; GONDRET, K.; BOIVIN, P. Evaluation of the Potential for Soil Organic Carbon Content Monitoring with Farmers. **Frontiers in Environmental Science** 8, 113, 2020.

FAO. Food and Agriculture Organization of the United Nations. **A protocol for measurement, monitoring, reporting and verification of soil organic carbon in agricultural landscapes - GSOC-MRV Protocol**. Rome, 2020a. Available in: https://doi.org/10.4060/cb0509en. Accessed on: 03 January 2021.

FAO. Food and Agriculture Organization of the United Nations. **Agricultura irrigada sustentável no Brasil: Identificação de áreas prioritárias**, 2017.

FAO. Food and Agriculture Organization of the United Nations. AQUASTAT: FAO's global information system on water and agriculture. Geospatial information, **Irrigation by country**, 2020b. Available in: http://www.fao.org/aquastat/en/geospatial-information/global-maps-irrigated-areas/irrigation-by-country. Accessed on: 28 December 2020.

FAO. Food and Agriculture Organization of the United Nations. **Global Agriculture Towards 2050**. High-Level Expert Forum: How to Feed the World in 2050, 2009.

FAO. Food and Agriculture Organization of the United Nations. **The irrigation challenge: Increasing irrigation contribution to food security through higher water productivity from canal irrigation systems**. Issues paper 4, 2003.

FRÓNA, D.; SZENDERÁK, J.; HARANGI-RÁKOS, M. The Challenge of Feeding the World. **Sustainability** 11, 20, 5816, 2019.

GHIMIRE, B.; GHIMIRE, R.; VANLEEUWEN, D.; MESBAH, A. Cover Crop Residue Amount and Quality Effects on Soil Organic Carbon Mineralization. **Sustainability** 9, 12, 2316, 2017.

HATFIELD, J. L.; DOLD, C. Water-use efficiency: Advances and challenges in a changing climate. **Frontiers in Plant Science** 10, 103, 2019.

JOHNSON, R.; CODY, B. A. **California Agricultural Production and Irrigated Water Use**. Congressional Research Service (CRS) Report, R44093, 2015. Available in: https://fas.org/sgp/crs/misc/R44093.pdf. Accessed on: 30 December 2020.

KENDALL, H. W., PIMENTEL, D. Constraints on the Expansion of the Global Food Supply. **Ambio** 23, 3, 198-205, 1994.

LAL, R. Soil Carbon Sequestration Impacts on Global Climate Change and Food Security. **Science** 304, 5677, 1623-1627, 2004.

LAL, R. Soil health and carbon management. **Food and Energy Security** 5, 4, 212-222, 2016.

MINASNY, B.; MCBRATNEY, A. B. Limited effect of organic matter on soil available water capacity. **European Journal of Soil Science** 69, 1, 39-47, 2017.

MIRCHOOLI, F.; KIANI-HARCHEGANI, M.; DARVISHAN, A. K.; FALAHATKAR, S.; SADEGHI, S. H. Spatial distribution dependency of soil organic carbon content to important environmental variables. **Ecological Indicators** 116, 106473, 2020.

MITCHELL, J. P.; SINGH, P. N.; WALLENDER, W. W.; MUNK, D. S.; WROBLE, J. F.; HORWATH, W. R.; HOGAN, P.; ROY, R.; HANSON, B. R. No-tillage and high-residue practices reduce soil water evaporation. **California Agriculture** 66, 55–61, 2012.

PATHAK, T.; MASKEY, M.; DAHLBERG, J.; KEARNS, F.; BALI, K.; ZACCARIA, D. Climate Change Trends and Impacts on California Agriculture: A Detailed Review. **Agronomy** 8, 3, 25, 2018.

PERRY, C.; STEDUTO, P.; ALLEN, R. G.; BURT, C. M. Increasing productivity in irrigated agriculture: Agronomic constraints and hydrological realities. **Agricultural Water Management** 96, 11, 1517-1524, 2009.

RUMPEL, C.; AMIRASLANI, F.; CHENU, C.; CARDENAS, M. G.; KAONGA, M.; KOUTIKA, L.; LADHA, J.; MADARI, B.; SHIRATO, Y.; SMITH, P.; SOUDI, B.; SOUSSANA, J. F.; WHITEHEAD, D.; WOLLENBERG, E. The 4p1000 initiative: Opportunities, limitations and challenges for implementing soil organic carbon sequestration as a sustainable development strategy. **Ambio** 49, 350-360, 2020.

SALAZAR, C.; RAND, J. Production risk and adoption of irrigation technology: evidence from small-scale farmers in Chile. **Latin American Economic Review** 25, 2, 2016.

SIEBERT, S.; HENRICH, V.; FRENKEN, K.; BURKE, J. **Update of the Digital Global Map of Irrigation Areas to Version 5**. Institute of Crop Science and Resource Conservation, Rheinische Friedrich-Wilhelms-Universität Bonn, Germany, 2013.

STELLA, T.; MOURATIADOU, I.; GAISER, T.; BERG-MOHNICKE, M.; WALLOR, E.; EWERT, F.; NENDEL, C. Estimating the contribution of crop residues to soil organic carbon conservation. **Environmental Research Letters** 14, 094008, 2019.

TESTEZLAF, R. **Irrigação: Métodos, sistemas e aplicações**. Campinas – SP: Unicamp/FEAGRI, 2017.

TURRAL H.; BURKE J.; FAURÈS J.-M. **Climate change, water and food security**. Food and Agriculture Organization of the United Nations (FAO), Water Reports 36. FAO, Rome, 2011.

UNITED NATIONS. Department of Economic and Social Affairs, Population Division. **World Population Prospects 2019: Highlights** (ST/ESA/SER.A/423), 2019.